Strange-Meson Spectroscopy – from COMPASS to AMBER

Stefan Wallner
for the COMPASS and AMBER collaborations
(swallner@mpp.mpg.de)

Max Planck Institute for Physics

XVth Quark Confinement and the Hadron Spectrum
August 5, 2022

COMPASS

AMBER
Apparatus for Meson and Baryon Experimental Research

MAX PLANCK INSTITUTE FOR PHYSICS

Understanding the light-meson spectrum

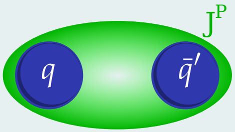

- Completing $\mathrm{SU(3)_{flavor}}$ multiplets
- Identifying supernumerous states
  - ➥ Search for exotic strange mesons

Input to other fields of physics

- Strange mesons appear as resonances in multi-body hadronic final states with kaons
- Searches for CP violation
- Searches for physics beyond SM

Understanding the light-meson spectrum

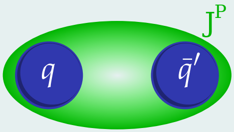

- Completing $\mathrm{SU}(3)_{\mathrm{flavor}}$ multiplets
- Identifying supernumerous states
  - ➥ Search for exotic strange mesons

Input to other fields of physics

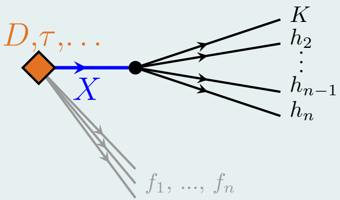

- Strange mesons appear as resonances in multi-body hadronic final states with kaons
- Searches for CP violation
- Searches for physics beyond SM

The Strange-Meson Spectrum

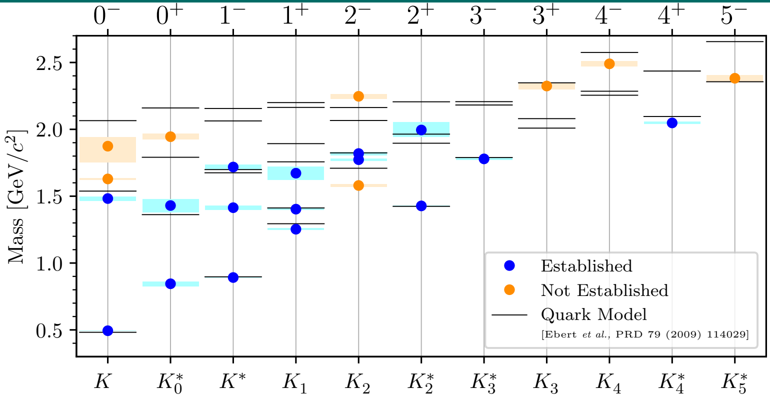

PDG lists 25 strange mesons (2021)

- 16 established states, 9 need further confirmation
- Missing states with respect to quark-model predictions
- Many measurements performed more than 30 years ago

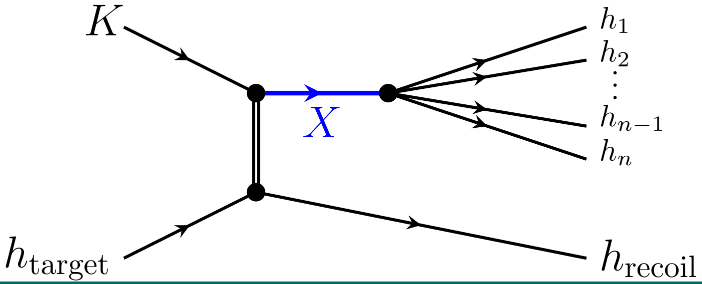

- Diffractive scattering of high-energy kaon beam
- Strange mesons appear as intermediate resonances X^-
- Decay to multi-body hadronic final states
- $K^-\pi^-\pi^+$ final state
  - Study in principle all strange mesons
  - Study a wide mass range
  - Study different decay modes

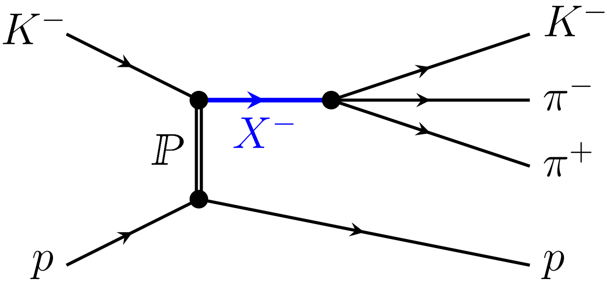

- Diffractive scattering of high-energy kaon beam
- Strange mesons appear as intermediate resonances X^-
- Decay to multi-body hadronic final states
- $K^-\pi^-\pi^+$ final state
  - Study in principle all strange mesons
  - Study a wide mass range
  - Study different decay modes

COMPASS Setup for Hadron Beams

[COMPASS, Nucl. Instrum. Methods **779** (2015) 69]

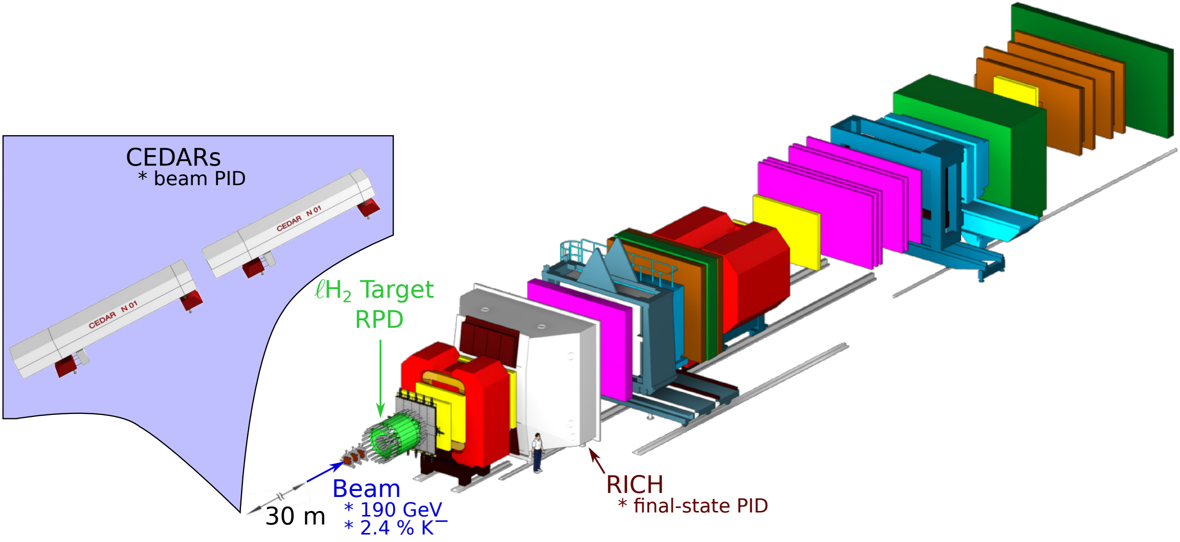

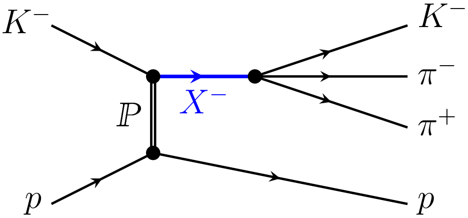

- World's largest data set of about 720 k events
- Rich spectrum of overlapping and interfering X^-
  - Dominant well known states
  - States with lower intensity are "hidden"

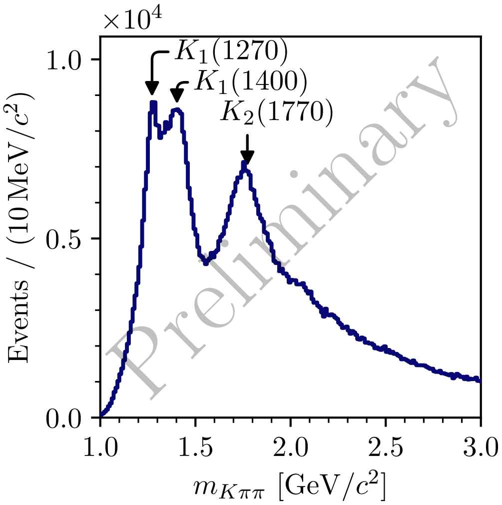

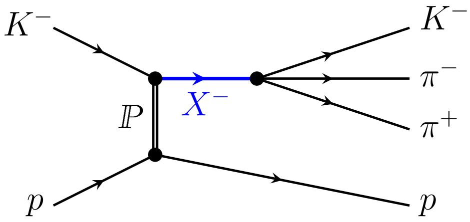

- World's largest data set of about 720 k events
- Rich spectrum of overlapping and interfering X^-
  - Dominant well known states
  - States with lower intensity are "hidden"

Partial wave: $J^P\, M^\varepsilon\, \xi\, b^-\, L$

- J^P spin and parity
- M^ε spin projection
- ξ isobar resonance
- b^- bachelor particle
- L orbital angular momentum

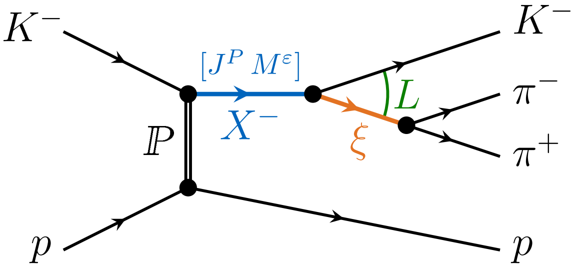

Partial wave: $J^P\ M^\varepsilon\ \xi\ b^-\ L$

- J^P spin and parity
- M^ε spin projection
- ξ isobar resonance
- b^- bachelor particle
- L orbital angular momentum

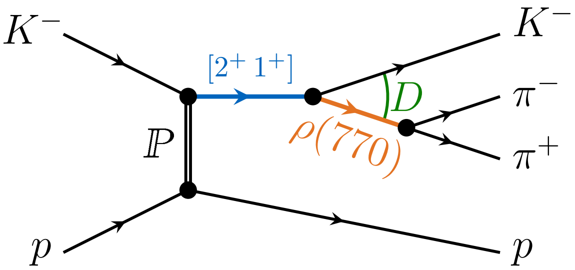

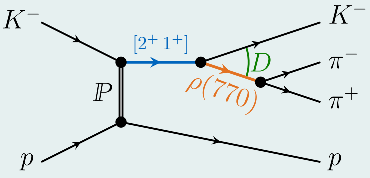

- Signal in $K_2^*(1430)$ mass region
- In different decays
  - $\rho(770)\ K\ D$
  - $K^*(892)\ \pi\ D$
- In agreement with previous measurements
- Cleaner signal in COMPASS data

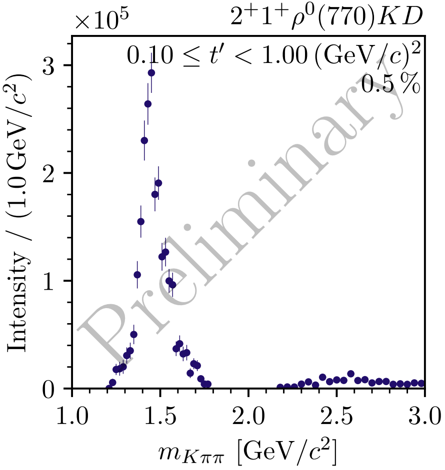

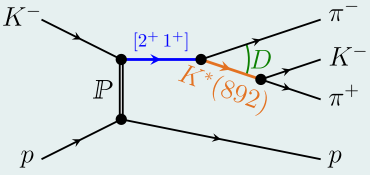

- Signal in $K_2^*(1430)$ mass region
- In different decays
  - $\rho(770)\, K\, D$
  - $K^*(892)\, \pi\, D$
- In agreement with previous measurements
- Cleaner signal in COMPASS data

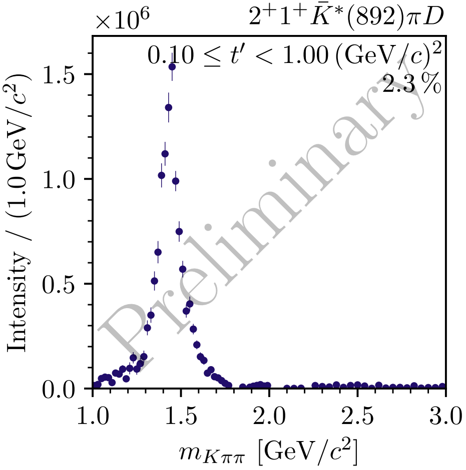

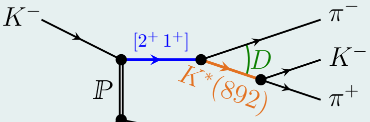

- Signal in $K_2^*(1430)$ mass region
- In different decays
  - $\rho(770)\,K\,D$
  - $K^*(892)\,\pi\,D$
- In agreement with previous measurements
- Cleaner signal in COMPASS data

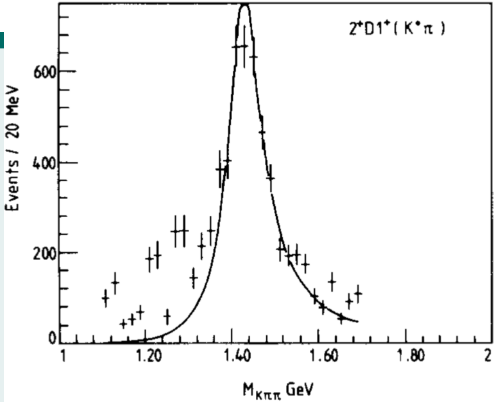

WA03 (CERN), 200 000 events, ACCMOR, Nucl. Phys. B **187** (1981)

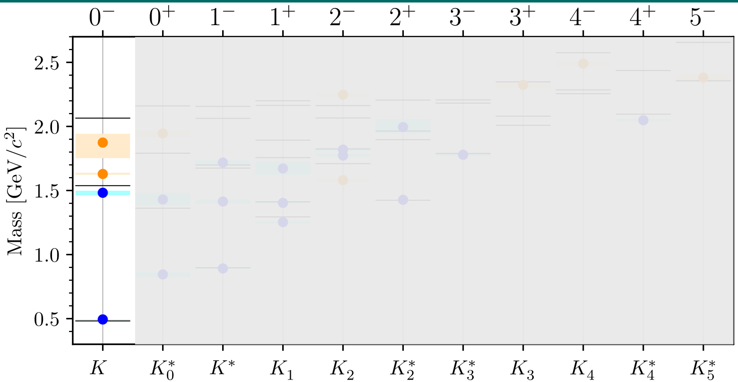

PDG

(2021)

- $K(1460)$ and $K(1830)$
- $K(1630)$
  - Unexpectedly small width of only 16 MeV/c^2
  - J^P of $K(1630)$ unclear

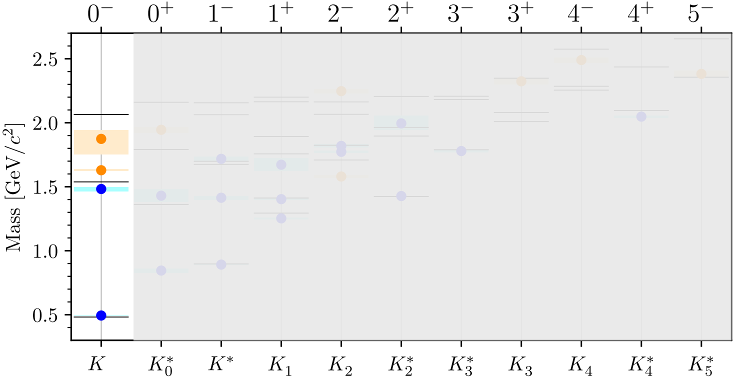

PDG

(2021)

- $K(1460)$ and $K(1830)$
- $K(1630)$
  - Unexpectedly small width of only 16 MeV/c^2
  - J^P of $K(1630)$ unclear

COMPASS $K^-\pi^-\pi^+$ data

- Peak at about 1.4 GeV/c^2
  - Potentially from established $K(1460)$
  - But, $m_{K\pi\pi} \lesssim 1.5$ GeV/c^2 region affected by analysis artifacts
- Second peak at about 1.7 GeV/c^2
  - Potential $K(1630)$ signal
  - Accompanied by clear phase motions
  - Width presumably larger than 16 MeV/c^2
- Weak signal at about 2.0 GeV/c^2
  - Potential $K(1830)$ signal

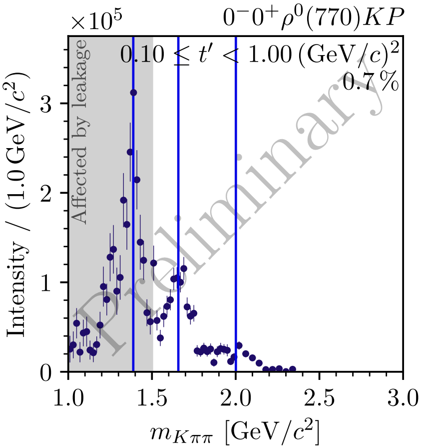

COMPASS $K^-\pi^-\pi^+$ data

- Peak at about $1.4\,\text{GeV}/c^2$
  - Potentially from established $K(1460)$
  - But, $m_{K\pi\pi} \lesssim 1.5\,\text{GeV}/c^2$ region affected by analysis artifacts
- Second peak at about $1.7\,\text{GeV}/c^2$
  - Potential $K(1630)$ signal
  - Accompanied by clear phase motions
  - Width presumably larger than $16\,\text{MeV}/c^2$
- Weak signal at about $2.0\,\text{GeV}/c^2$
  - Potential $K(1830)$ signal

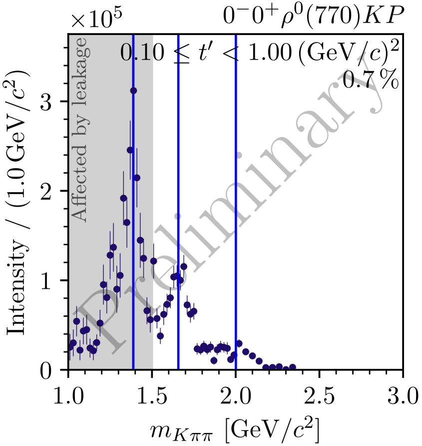

COMPASS $K^-\pi^-\pi^+$ data

- Peak at about 1.4 GeV/c^2
  - Potentially from established $K(1460)$
  - But, $m_{K\pi\pi} \lesssim 1.5\,\text{GeV}/c^2$ region affected by analysis artifacts
- Second peak at about 1.7 GeV/c^2
  - Potential $K(1630)$ signal
  - Accompanied by clear phase motions
  - Width presumably larger than 16 MeV/c^2
- Weak signal at about 2.0 GeV/c^2
  - Potential $K(1830)$ signal

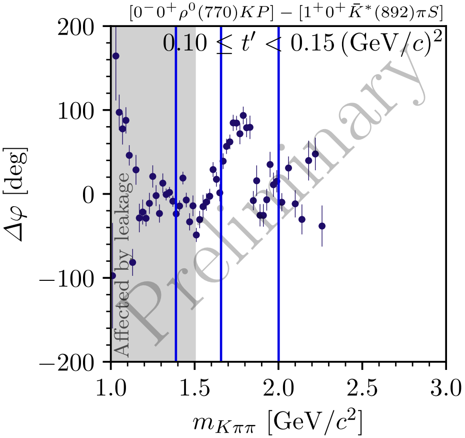

COMPASS $K^-\pi^-\pi^+$ data

- Peak at about 1.4 GeV/c^2
  - Potentially from established $K(1460)$
  - But, $m_{K\pi\pi} \lesssim 1.5$ GeV/c^2 region affected by analysis artifacts
- Second peak at about 1.7 GeV/c^2
  - Potential $K(1630)$ signal
  - Accompanied by clear phase motions
  - Width presumably larger than 16 MeV/c^2
- Weak signal at about 2.0 GeV/c^2
  - Potential $K(1830)$ signal

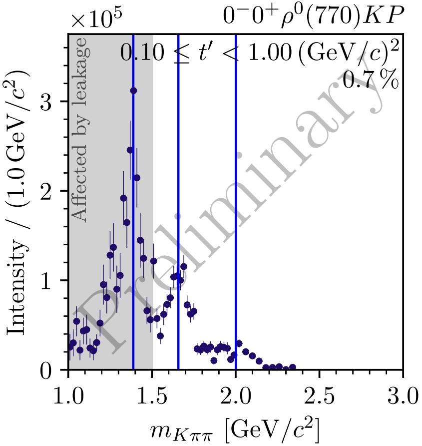

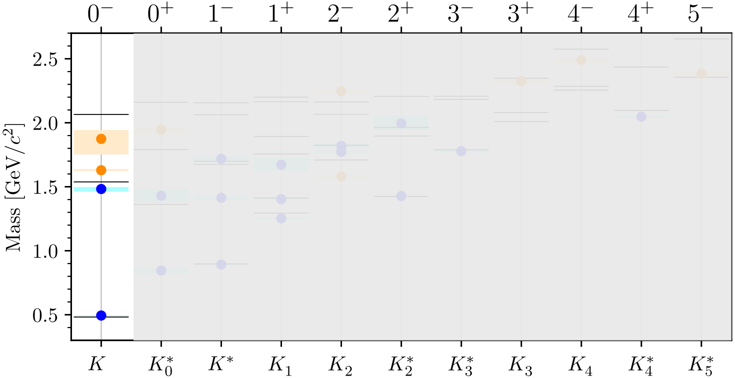

- Indications for 3 excited K from a single analysis
- Quark-model predicts only two excited states: potentially $K(1460)$ and $K(1830)$
  - ➥ $K(1630)$ supernumerary state
  - ➥ Candidate for exotic non-$q\bar{q}$ state

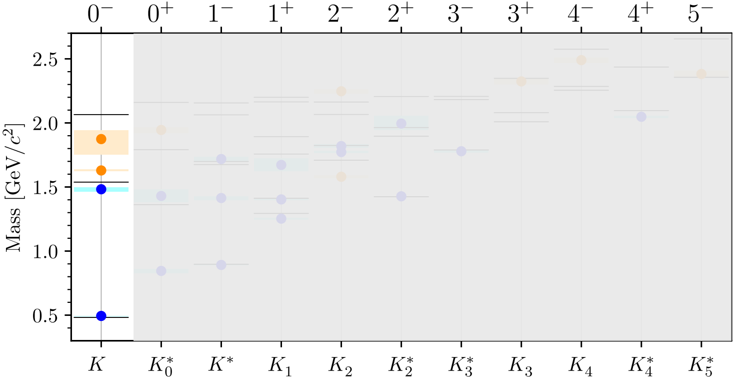

- Indications for 3 excited K from a single analysis
- Quark-model predicts only two excited states: potentially $K(1460)$ and $K(1830)$
  - ➥ $K(1630)$ supernumerary state
  - ➥ Candidate for exotic non-$q\bar{q}$ state

- Final-state particle identification does not cover full momentum range
  - ➥ Loss of distinguishing power for some partial waves
  - ➥ Analysis artifacts in these partial waves

- Artifacts can be identified
- Mainly affects only
  - a sub-set of partial waves
  - the range $m_{K\pi\pi} \lesssim 1.6\,\mathrm{GeV}/c^2$

- Limits access to certain decay modes
- Induces non-negligible systematic uncertainties

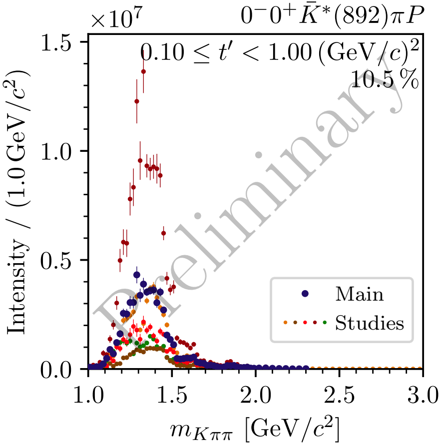

- Final-state particle identification does not cover full momentum range
  - ➥ Loss of distinguishing power for some partial waves
  - ➥ Analysis artifacts in these partial waves

- Artifacts can be identified
- Mainly affects only
  - a sub-set of partial waves
  - the range $m_{K\pi\pi} \lesssim 1.6\,\text{GeV}/c^2$

- Limits access to certain decay modes
- Induces non-negligible systematic uncertainties

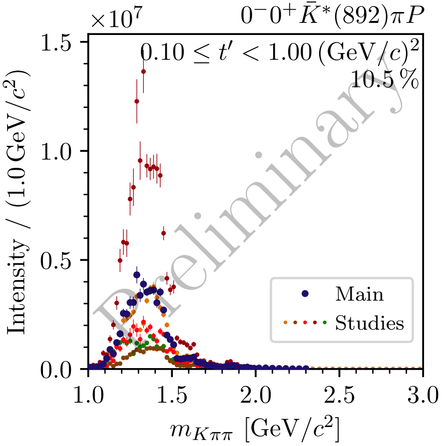

- Final-state particle identification does not cover full momentum range
  - ➡ Loss of distinguishing power for some partial waves
  - ➡ Analysis artifacts in these partial waves

- Artifacts can be identified
- Mainly affects only
  - a sub-set of partial waves
  - the range $m_{K\pi\pi} \lesssim 1.6\,\text{GeV}/c^2$

- Limits access to certain decay modes
- Induces non-negligible systematic uncertainties

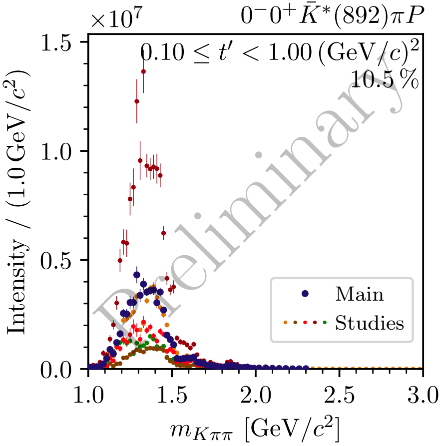

Limitations for Strange-Meson Spectroscopy at COMPASS

Main limiting factors

- Final-state particle identification
- Size of the data samples
    - Low kaon fraction in the beam ($\approx 2\,\%$)
    - Sample for strange-mesons about 150-times smaller than sample for non-strange mesons
        - 720 k $K^- + p \to K^-\pi^-\pi^+ + p$ events
        - 115 M $\pi^- + p \to \pi^-\pi^-\pi^+ + p$ events

AMBER

Apparatus for Meson and Baryon Experimental Research

Phase I: After long shutdown 2 of LHC [CERN-SPSC-2019-022]

- Proton charge-radius measurement
- Drell-Yan and charmonium production
- p-induced $\bar{p}$ production cross section

Phase II: After long shutdown 3 of LHC [arXiv:1808.00848]

- Physics with kaon beams
  - Strange-meson spectroscopy
    goal: $10\times$ larger data sample
  - Kaon-induced charmonium production
  - ...
- ...

Key Requirements for the Experimental Setup

- Upgrade of final-state particle identification
  - Cover wide momentum range
  - Large and uniform acceptance
- Efficient beam-particle identification for high-purity sample
- High-resolution track reconstruction
- Efficient photon detection for access to final states with neutral particles

- Eliminate artifacts caused by limited final-state particle identification
- Increase size of the data sample by increasing acceptance

- Increase size of the data sample by increasing kaon fraction in beam

Radio-frequency separation

- Particle species discrimination by time-of-flight
  - Same momentum
  - But different velocity
- Transverse kick by RF cavities
- Kick by RF1 compensated or amplified by RF2, depending on phase (velocity)
- Feasibility studies ongoing

- Increase size of the data sample by increasing kaon fraction in beam

Radio-frequency separation

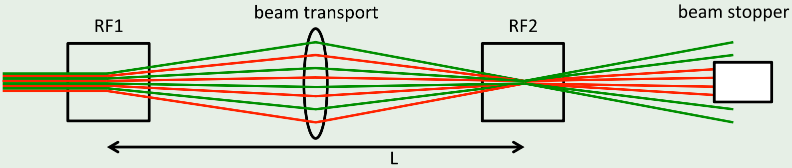

- Particle species discrimination by time-of-flight
  - Same momentum
  - But different velocity
- Transverse kick by RF cavities
- Kick by RF1 compensated or amplified by RF2, depending on phase (velocity)
- Feasibility studies ongoing

The virtue of larger data samples

- Improved precision
- Study also small signals in data
- Access to novel analysis methods

Freed-isobar partial-wave analysis

- K_0^* mesons ($J^P = 0^+$) cannot be directly produced in diffractive scattering
- K_0^* mesons appear in $K^-\pi^+$ sub-system of the $K^-\pi^-\pi^+$ final state
- Freed-isobar method allows us to study mesons in sub-systems
  - Developed and successfully applied to COMPASS $\pi^-\pi^-\pi^+$ sample
  - Requires large data samples

The virtue of larger data samples

- Improved precision
- Study also small signals in data
- Access to novel analysis methods

Freed-isobar partial-wave analysis

- K_0^* mesons ($J^P = 0^+$) cannot be directly produced in diffractive scattering
- K_0^* mesons appear in $K^-\pi^+$ sub-system of the $K^-\pi^-\pi^+$ final state
- Freed-isobar method allows us to study mesons in sub-systems
  - Developed and successfully applied to COMPASS $\pi^-\pi^-\pi^+$ sample
  - Requires large data samples

The virtue of larger data samples

- Improved precision
- Study also small signals in data
- Access to novel analysis methods

Freed-isobar partial-wave analysis

- K_0^* mesons ($J^P = 0^+$) cannot be directly produced in diffractive scattering
- K_0^* mesons appear in $K^-\pi^+$ sub-system of the $K^-\pi^-\pi^+$ final state
- Freed-isobar method allows us to study mesons in sub-systems
  - Developed and successfully applied to COMPASS $\pi^-\pi^-\pi^+$ sample
  - Requires large data samples

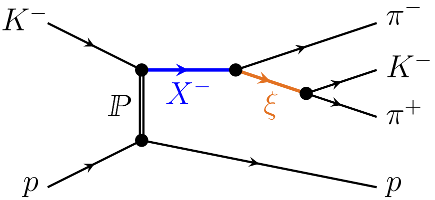

Summary

The Strange-Meson Spectrum

- Many strange mesons require further confirmation
- Search for strange partners of exotic non-strange light mesons

COMPASS

- World's largest data sample on $K^- + p \to K^-\pi^-\pi^+ + p$
  - Most detailed and comprehensive analysis of the $K^-\pi^-\pi^+$ final state so far
- Limited by final-state particle identification and small kaon fraction in beam

AMBER: High-Precision Strange-Meson Spectroscopy

- Goal: Collect 10×larger sample using high-intensity and high-energy kaon beam
- Rewrite the PDG for strange mesons, with a single and self-consistent measurement
- Requires experimental setup with uniform acceptance over wide kinematic range including particle identification and measurement of neutral particles
- AMBER is open for interested collaborators to join

Summary

The Strange-Meson Spectrum

- Many strange mesons require further confirmation
- Search for strange partners of exotic non-strange light mesons

COMPASS

- World's largest data sample on $K^- + p \to K^-\pi^-\pi^+ + p$
  - Most detailed and comprehensive analysis of the $K^-\pi^-\pi^+$ final state so far
- Limited by final-state particle identification and small kaon fraction in beam

AMBER: High-Precision Strange-Meson Spectroscopy

- Goal: Collect $10\times$larger sample using high-intensity and high-energy kaon beam
- Rewrite the PDG for strange mesons, with a single and self-consistent measurement
- Requires experimental setup with uniform acceptance over wide kinematic range including particle identification and measurement of neutral particles
- AMBER is open for interested collaborators to join

Summary

The Strange-Meson Spectrum

- Many strange mesons require further confirmation
- Search for strange partners of exotic non-strange light mesons

COMPASS

- World's largest data sample on $K^- + p \to K^-\pi^-\pi^+ + p$
  - Most detailed and comprehensive analysis of the $K^-\pi^-\pi^+$ final state so far
- Limited by final-state particle identification and small kaon fraction in beam

AMBER: High-Precision Strange-Meson Spectroscopy

- Goal: Collect 10×larger sample using high-intensity and high-energy kaon beam
- Rewrite the PDG for strange mesons, with a single and self-consistent measurement
- Requires experimental setup with uniform acceptance over wide kinematic range including particle identification and measurement of neutral particles
- AMBER is open for interested collaborators to join

Backup

Outline

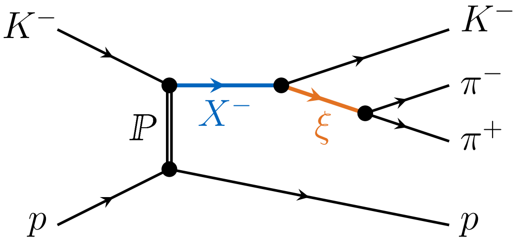

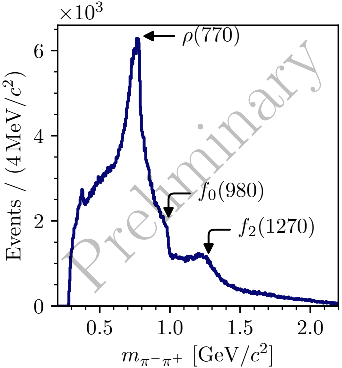

- Also structure in $\pi^-\pi^+$ and $K^-\pi^+$ subsystems
  - ➥ Successive 2-body decay via $\pi^-\pi^+$ / $K^-\pi^+$ resonance called isobar
- Also structure in angular distributions

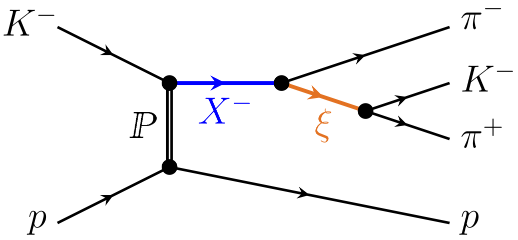

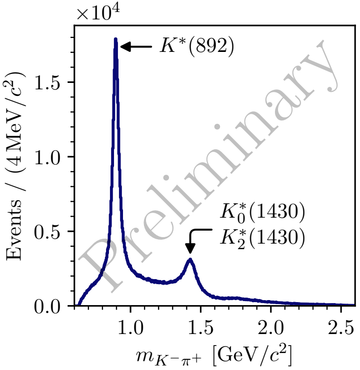

- Also structure in $\pi^-\pi^+$ and $K^-\pi^+$ subsystems
  - ➥ Successive 2-body decay via $\pi^-\pi^+$ / $K^-\pi^+$ resonance called isobar
- Also structure in angular distributions

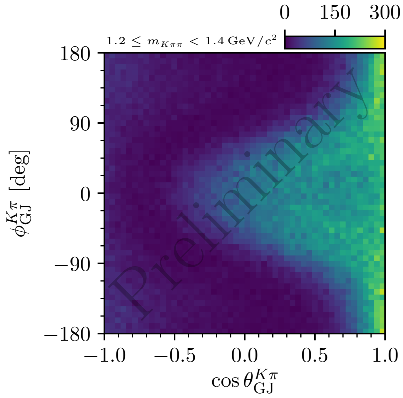

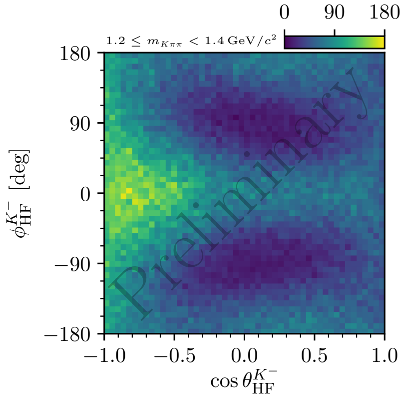

- Also structure in $\pi^-\pi^+$ and $K^-\pi^+$ subsystems
  - ➥ Successive 2-body decay via $\pi^-\pi^+$ / $K^-\pi^+$ resonance called isobar
- Also structure in angular distributions

- No dominant resonant structures

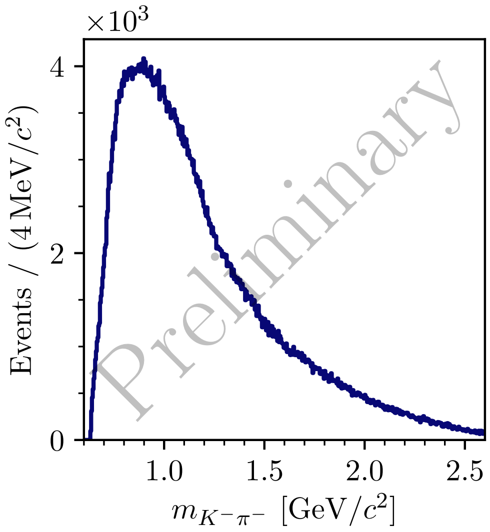

- Exponential shape
- Shallower for larger t'

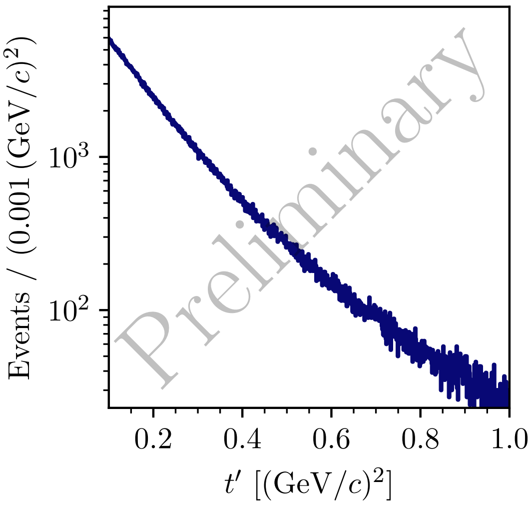

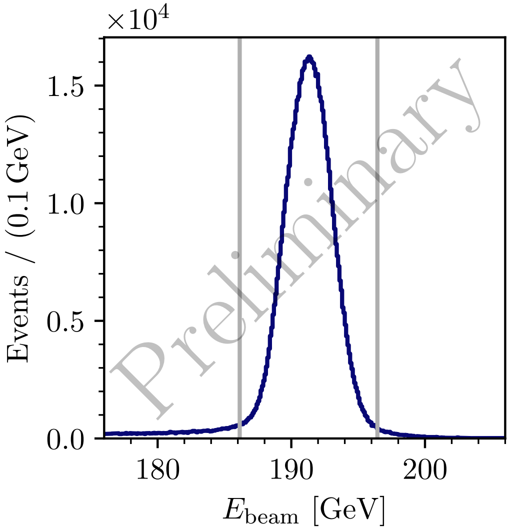
×10^4
1.5
1.0
0.5
0.0
Events / (0.1 GeV)
180
190
200
E_{beam} [GeV]
Preliminary

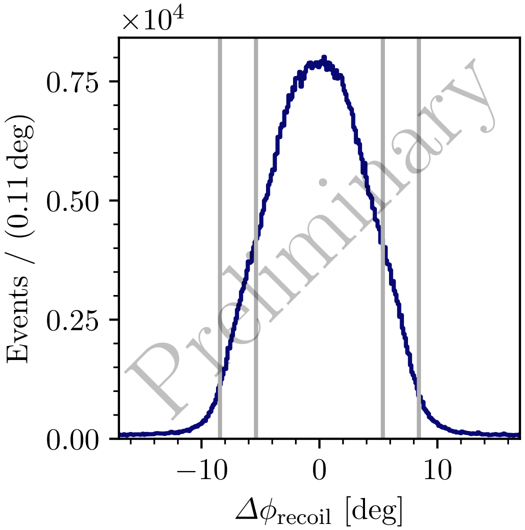
×10^4
0.75
0.50
0.25
0.00
Events / (0.11 deg)
−10
0
10
$\Delta\phi_{\mathrm{recoil}}$ [deg]
Preliminary

Kinematic Distribution of $K^-\pi^-\pi^+$ Events
Exclusivity

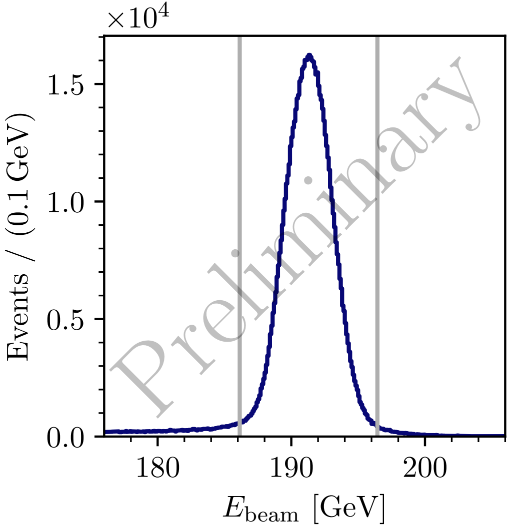

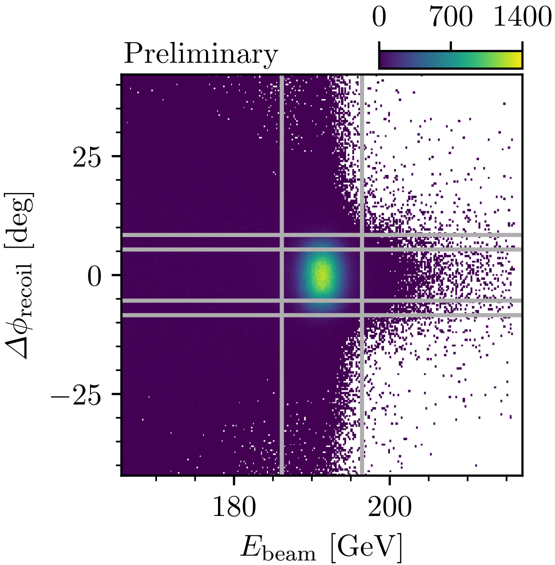

Partial waves with $J^P = 2^+$

- Signal in $K_2^*(1430)$ mass region
- In Different decays
  - $\rho(770)\ K\ D$
  - $K^*(892)\ \pi\ D$
- Clear phase motion in $K_2^*(1430)$ region
  - Characteristic of narrow isolated resonances
- In agreement with previous measurement

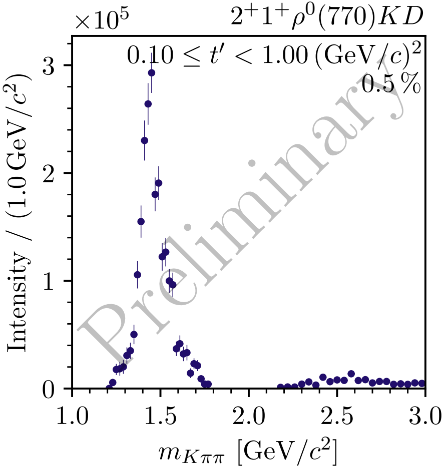

Partial waves with $J^P = 2^+$

- Signal in $K_2^*(1430)$ mass region
- In Different decays
  - $\rho(770)\,K\,D$
  - $K^*(892)\,\pi\,D$
- Clear phase motion in $K_2^*(1430)$ region
  - Characteristic of narrow isolated resonances
- In agreement with previous measurement

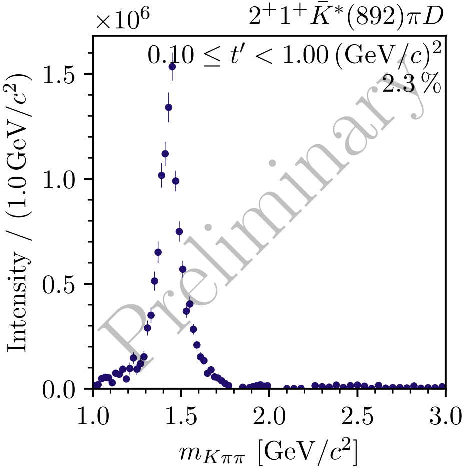

Partial waves with $J^P = 2^+$

- Signal in $K_2^*(1430)$ mass region
- In Different decays
  - $\rho(770)\,K\,D$
  - $K^*(892)\,\pi\,D$
- Clear phase motion in $K_2^*(1430)$ region
  - Characteristic of narrow isolated resonances
- In agreement with previous measurement

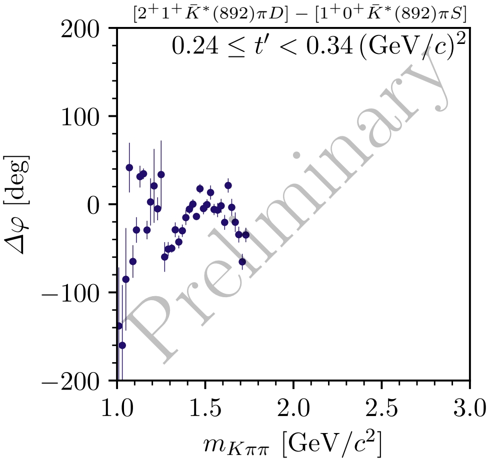

Partial waves with $J^P = 2^+$

- Signal in $K_2^*(1430)$ mass region
- In Different decays
  - $\rho(770)\,K\,D$
  - $K^*(892)\,\pi\,D$
- Clear phase motion in $K_2^*(1430)$ region
  - Characteristic of narrow isolated resonances
- In agreement with previous measurement

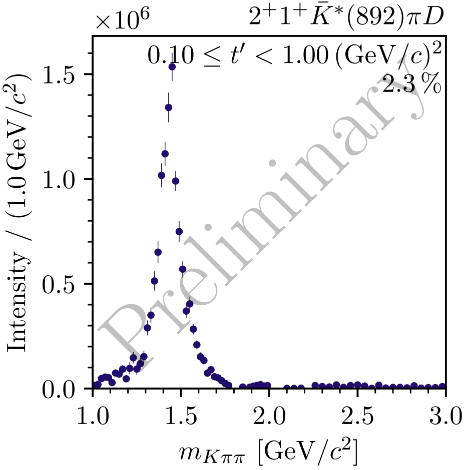

WA03 (CERN), 200 000 events, ACCMOR, Nucl. Phys. B **187** (1981)

Partial waves with $J^P = 2^+$

- Signal in $K_2^*(1430)$ mass region
- In Different decays
  - $\rho(770)\, K\, D$
  - $K^*(892)\, \pi\, D$
- Clear phase motion in $K_2^*(1430)$ region
  - Characteristic of narrow isolated resonances
- In agreement with previous measurement

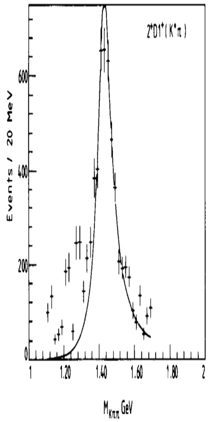

WA03 (CERN), 200 000 events, ACCMOR, Nucl. Phys. B **187** (1981)

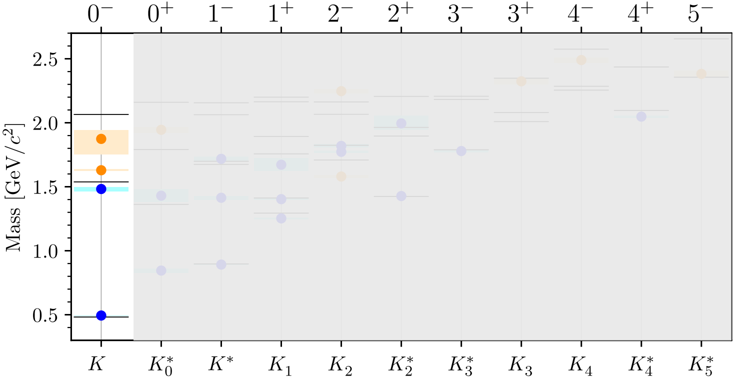

PDG (2021)

- $K(1460)$ and $K(1830)$ potentially quark-model states
- $K(1630)$ candidate for supernumerary state
  - Unexpectedly small width: 16 MeV/c^2
  - J^P of $K(1630)$ unclear

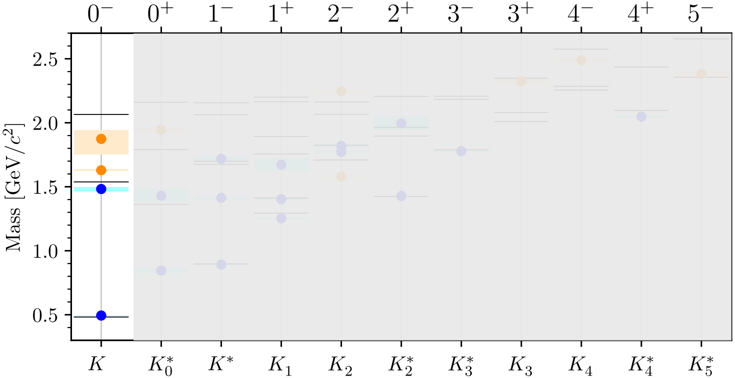

PDG (2021)

- $K(1460)$ and $K(1830)$ potentially quark-model states
- $K(1630)$ candidate for supernumerary state
  - Unexpectedly small width: 16 MeV/c^2
  - J^P of $K(1630)$ unclear

$0^-\ 0^+\ \rho(770)\ K\ P$ partial wave

- Peak at about $1.4\,\text{GeV}/c^2$
  - Potentially from established $K(1460)$
  - $m \lesssim 1.5\,\text{GeV}/c^2$ region affected by analysis artifacts
- Second peak at about $1.7\,\text{GeV}/c^2$
  - Potential $K(1630)$ signal
  - Accompanied by clear phase motion
  - Width presumably larger than $16\,\text{MeV}/c^2$

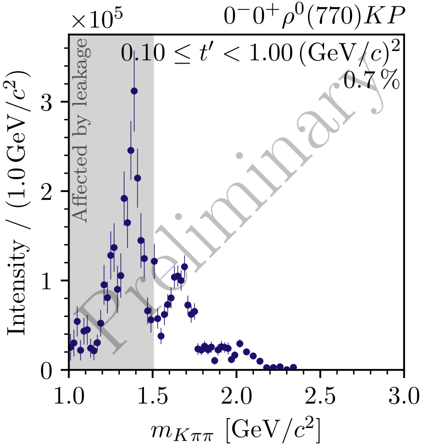

$0^-\ 0^+\ \rho(770)\ K\ P$ partial wave

- Peak at about $1.4\,\mathrm{GeV}/c^2$
  - Potentially from established $K(1460)$
  - $m \lesssim 1.5\,\mathrm{GeV}/c^2$ region affected by analysis artifacts
- Second peak at about $1.7\,\mathrm{GeV}/c^2$
  - Potential $K(1630)$ signal
  - Accompanied by clear phase motion
  - Width presumably larger than $16\,\mathrm{MeV}/c^2$

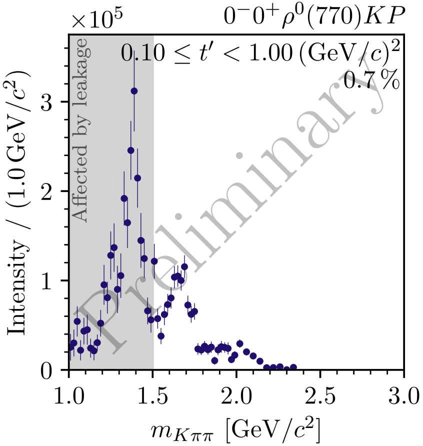

$0^-\ 0^+\ \rho(770)\ K\ P$ partial wave

- Peak at about 1.4 GeV/c^2
  - Potentially from established $K(1460)$
  - $m \lesssim 1.5$ GeV/c^2 region affected by analysis artifacts
- Second peak at about 1.7 GeV/c^2
  - Potential $K(1630)$ signal
  - Accompanied by clear phase motion
  - Width presumably larger than 16 MeV/c^2

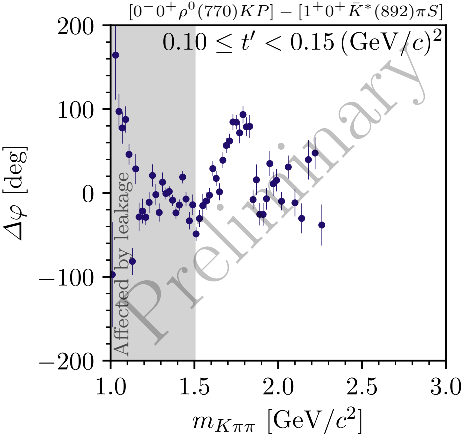

Partial Waves with $J^P = 0^-$

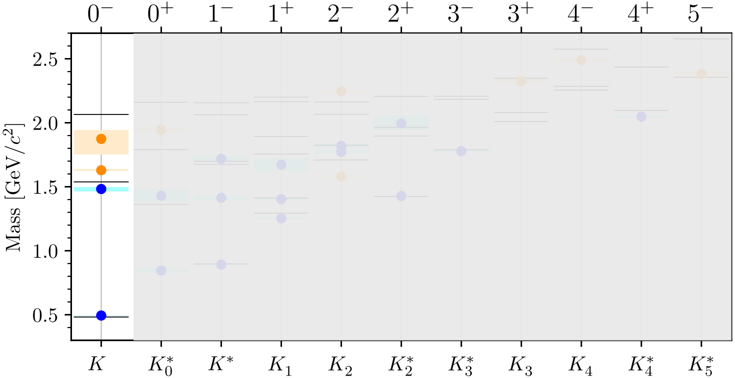

PDG

(2021)

- $K(1460)$ and $K(1830)$
- $K(1630)$
  - Unexpectedly small width: 16 MeV/c^2
  - J^P of $K(1630)$ unclear

Partial Waves with $J^P = 0^-$

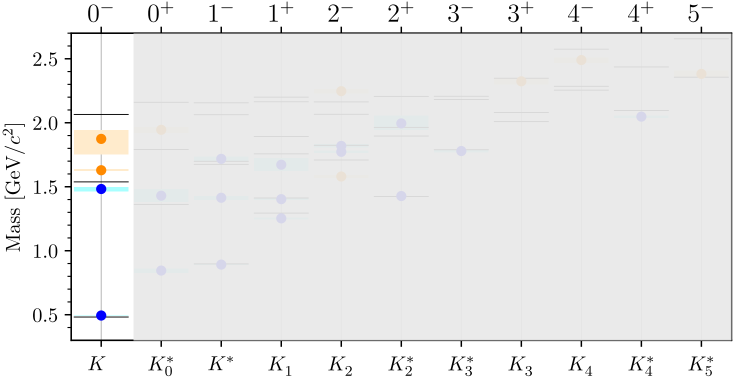

PDG

(2021)

- $K(1460)$ and $K(1830)$
- $K(1630)$
  - Unexpectedly small width: 16 MeV$/c^2$
  - J^P of $K(1630)$ unclear

Partial Waves with $J^P = 0^-$

$K^-\pi^-\pi^+$ from COMPASS

- Peak at about 1.4 GeV$/c^2$
  - Potentially from established $K(1460)$
  - But, $m \lesssim 1.5$ GeV$/c^2$ region affected by analysis artifacts
- Second peak at about 1.7 GeV$/c^2$
  - Potential $K(1630)$ signal
  - Accompanied by clear phase motion
  - Width presumably larger than 16 MeV$/c^2$

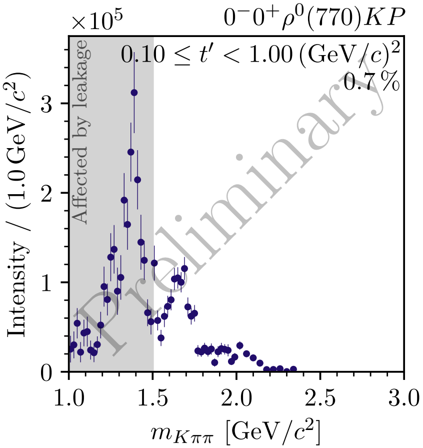

$K^- \pi^- \pi^+$ from COMPASS

- Peak at about 1.4 GeV/c^2
  - Potentially from established $K(1460)$
  - But, $m \lesssim 1.5$ GeV/c^2 region affected by analysis artifacts
- Second peak at about 1.7 GeV/c^2
  - Potential $K(1630)$ signal
  - Accompanied by clear phase motion
  - Width presumably larger than 16 MeV/c^2

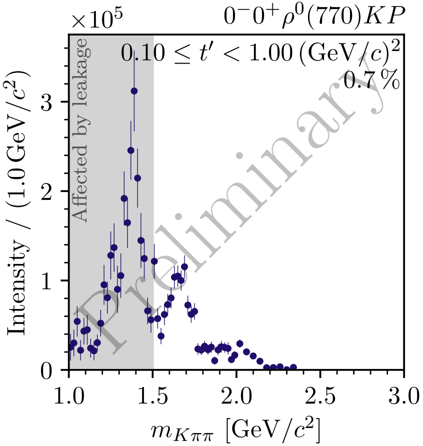

$K^-\pi^-\pi^+$ from COMPASS

- Peak at about 1.4 GeV/c^2
  - Potentially from established $K(1460)$
  - But, $m \lesssim 1.5$ GeV/c^2 region affected by analysis artifacts
- Second peak at about 1.7 GeV/c^2
  - Potential $K(1630)$ signal
  - Accompanied by clear phase motion
  - Width presumably larger than 16 MeV/c^2

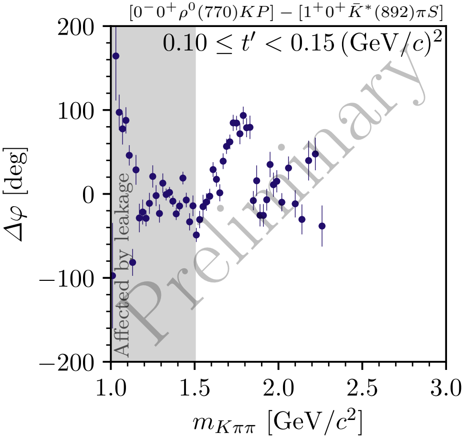

Partial Waves with $J^P = 0^-$

$K^-\pi^-\pi^+$ from ACCMOR

- Potential $K(1630)$ signal already in ACCMOR analysis

$K^-\pi^-\pi^+$ from LHCb

- Measurement of $D^0 \to K^\mp\pi^\pm\pi^\pm\pi^\mp$ at LHCb
  - Study strange mesons in $K\pi\pi$ subsystem
  - MIPWA of $J^P = 0^-$ amplitude
  - Potential signal above 1.6 GeV/c^2
  - Limited by kinematic range

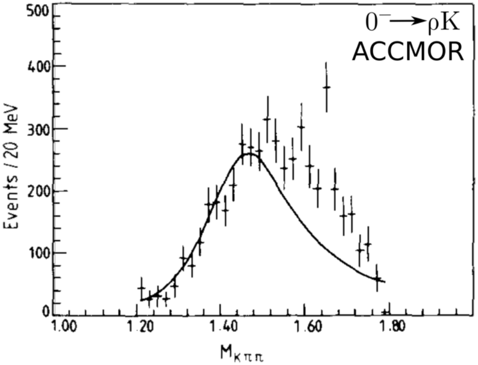

WA03 (CERN), 200 000 events, ACCMOR, Nucl. Phys. B **187** (1981)

Partial Waves with $J^P = 0^-$

$K^-\pi^-\pi^+$ from ACCMOR

- Potential $K(1630)$ signal already in ACCMOR analysis

$K^-\pi^-\pi^+$ from LHCb

- Measurement of $D^0 \to K^\mp\pi^\pm\pi^\pm\pi^\mp$ at LHCb
  - Study strange mesons in $K\pi\pi$ subsystem
  - MIPWA of $J^P = 0^-$ amplitude
  - Potential signal above $1.6\,\mathrm{GeV}/c^2$
  - Limited by kinematic range

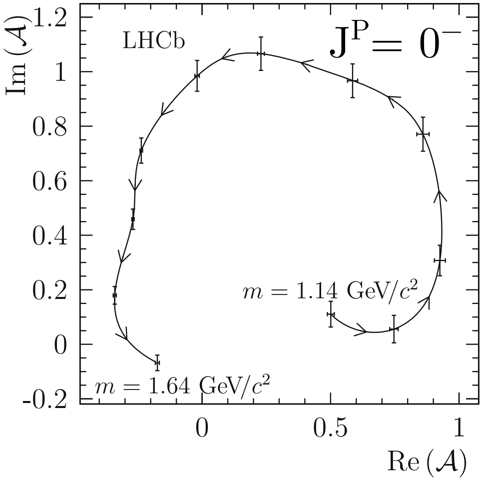

LHCb, 893 000 events, Eur. Phys. J. C **78** (2018)

Partial Waves with $J^P = 0^-$

$K^-\pi^-\pi^+$ from ACCMOR

- Potential $K(1630)$ signal already in ACCMOR analysis

$K^-\pi^-\pi^+$ from LHCb

- Measurement of $D^0 \to K^\mp\pi^\pm\pi^\pm\pi^\mp$ at LHCb
  - Study strange mesons in $K\pi\pi$ subsystem
  - MIPWA of $J^P = 0^-$ amplitude
  - Potential signal above 1.6 GeV/c^2
  - Limited by kinematic range

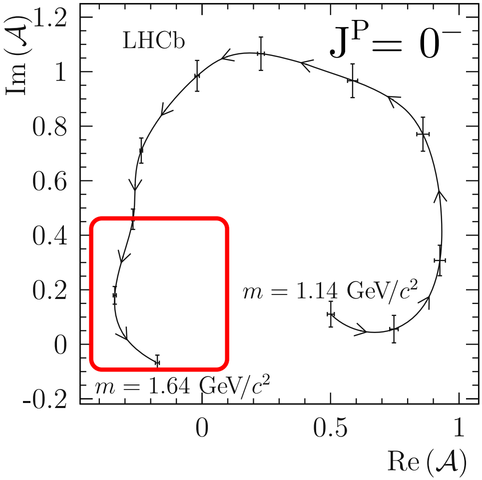

LHCb, 893 000 events, Eur. Phys. J. C **78** (2018)

Partial Waves with $J^P = 0^-$

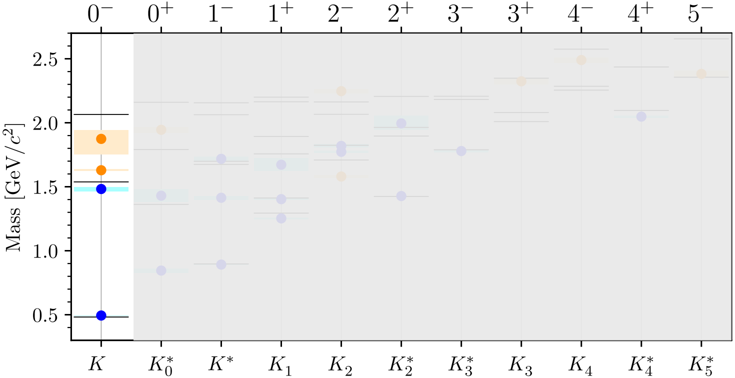

- Indications for 3 excited K from a single analysis
- Quark-model predicts only two excited states: $K(1460)$ and $K(1830)$ potentially quark-model states
  - ➥ Supernumerary state
  - ➥ $K(1630)$ candidate for exotic non-$q\bar{q}$ state

Partial Waves with $J^P = 0^-$

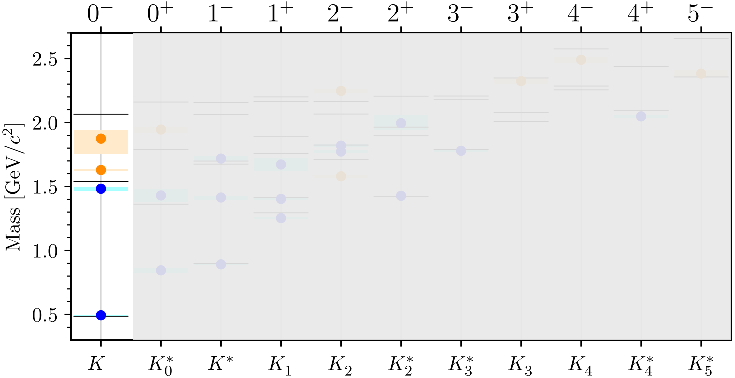

- Indications for 3 excited K from a single analysis
- Quark-model predicts only two excited states: $K(1460)$ and $K(1830)$ potentially quark-model states
  - ➥ Supernumerary state
  - ➥ $K(1630)$ candidate for exotic non-$q\bar{q}$ state

Partial Waves with $J^P = 0^-$

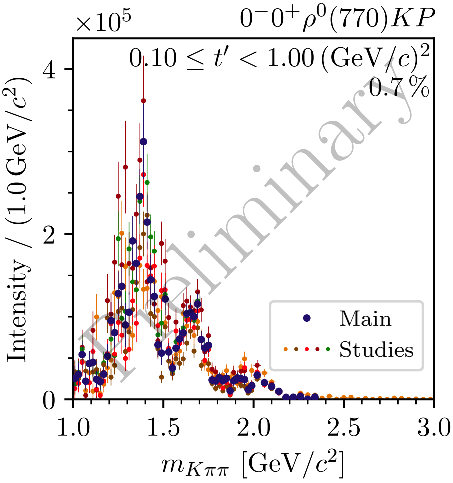

Leakage Effect

- Unexpected low-mass enhancement in $3^+ 1^+$ $K^*(892)\,\pi\,D$ wave
- Similar to dominant 1^+ wave
- Sensitive to systematic effects
- Decay amplitudes of different J^P are orthogonal
- Loss of orthogonality taking acceptance into account
- Limited acceptance due to limited kinematic range of final-state PID
- Only a small sub-set of partial waves affected

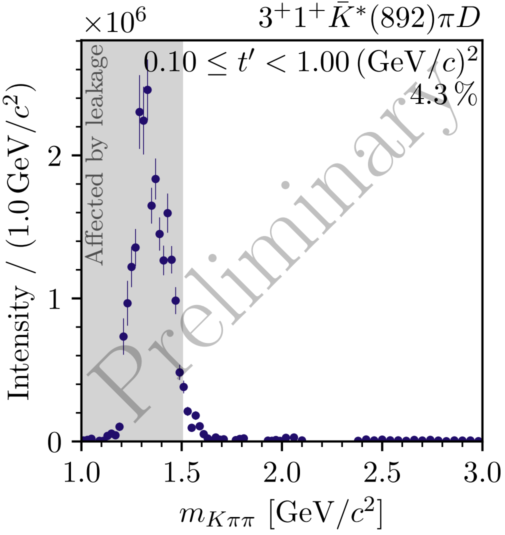

Leakage Effect

- Unexpected low-mass enhancement in $3^{+}\,1^{+}\,K^{*}(892)\,\pi\,D$ wave
- Similar to dominant 1^{+} wave
- Sensitive to systematic effects
- Decay amplitudes of different J^{P} are orthogonal
- Loss of orthogonality taking acceptance into account
- Limited acceptance due to limited kinematic range of final-state PID
- Only a small sub-set of partial waves affected

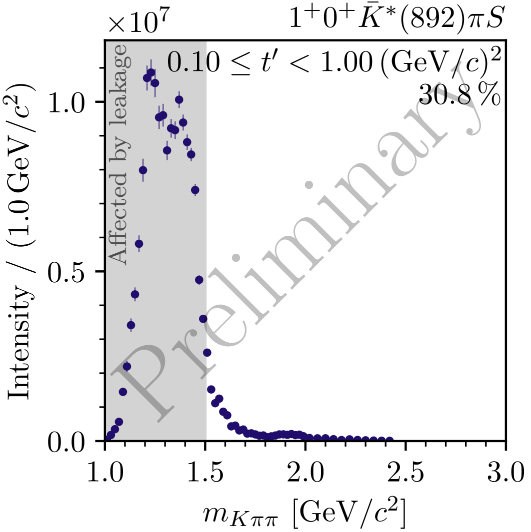

Leakage Effect

- Unexpected low-mass enhancement in $3^+\,1^+$ $K^*(892)\,\pi\,D$ wave
- Similar to dominant 1^+ wave
- Sensitive to systematic effects
- Decay amplitudes of different J^P are orthogonal
- Loss of orthogonality taking acceptance into account
- Limited acceptance due to limited kinematic range of final-state PID
- Only a small sub-set of partial waves affected

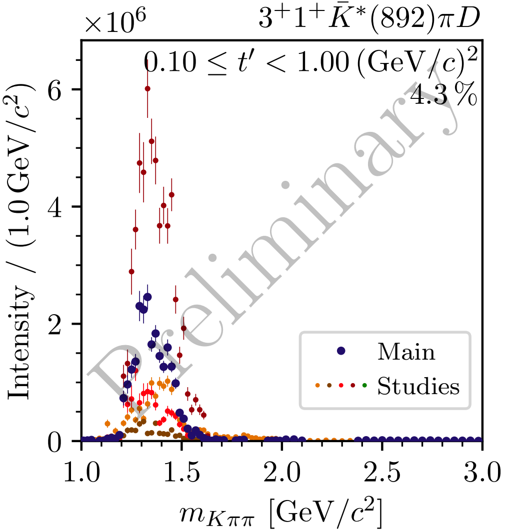

Leakage Effect

- Unexpected low-mass enhancement in $3^+ 1^+$ $K^*(892)\,\pi\ D$ wave
- Similar to dominant 1^+ wave
- Sensitive to systematic effects
- Decay amplitudes of different J^P are orthogonal
- Loss of orthogonality taking acceptance into account
- Limited acceptance due to limited kinematic range of final-state PID
- Only a small sub-set of partial waves affected

$$I_{a,b} = \int \mathrm{d}\varphi_3(\tau)\ \Psi_a(\tau)\Psi_b^*(\tau)$$

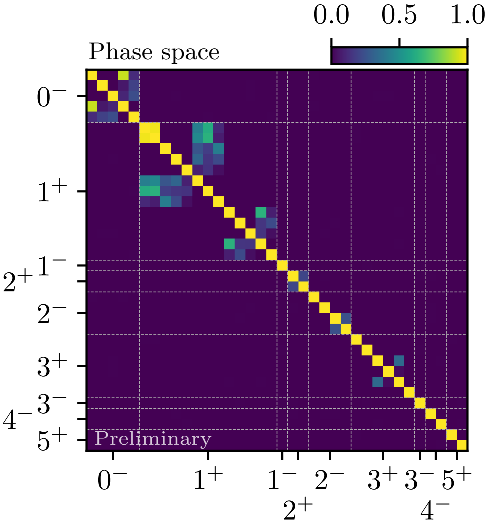

Leakage Effect

- Unexpected low-mass enhancement in $3^+\,1^+$ $K^*(892)\,\pi\,D$ wave
- Similar to dominant 1^+ wave
- Sensitive to systematic effects
- Decay amplitudes of different J^P are orthogonal
- Loss of orthogonality taking acceptance into account
- Limited acceptance due to limited kinematic range of final-state PID
- Only a small sub-set of partial waves affected

$$\bar{I}_{a,b} = \int \mathrm{d}\varphi_3(\tau)\ \eta(\tau)\ \Psi_a(\tau)\Psi_b^*(\tau)$$

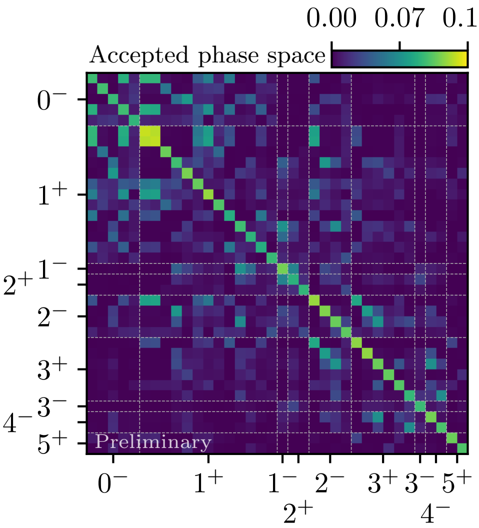

Leakage Effect

- Unexpected low-mass enhancement in $3^+ 1^+$ $K^*(892)\,\pi\, D$ wave
- Similar to dominant 1^+ wave
- Sensitive to systematic effects
- Decay amplitudes of different J^P are orthogonal
- Loss of orthogonality taking acceptance into account
- Limited acceptance due to limited kinematic range of final-state PID
- Only a small sub-set of partial waves affected

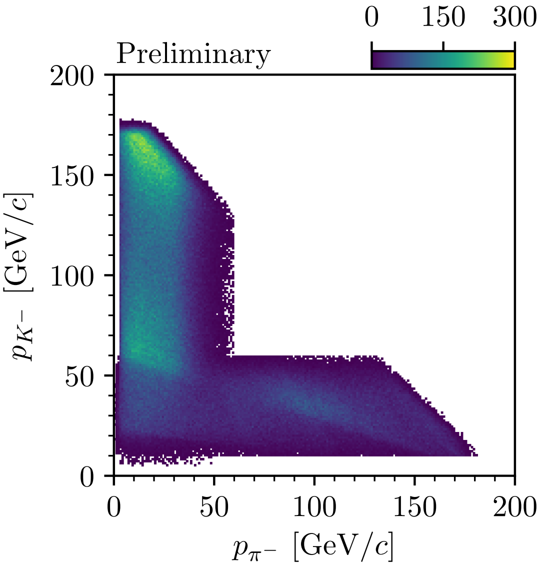

Leakage Effect

- Unexpected low-mass enhancement in $3^+ 1^+ K^*(892)\,\pi\, D$ wave
- Similar to dominant 1^+ wave
- Sensitive to systematic effects
- Decay amplitudes of different J^P are orthogonal
- Loss of orthogonality taking acceptance into account
- Limited acceptance due to limited kinematic range of final-state PID
- Only a small sub-set of partial waves affected

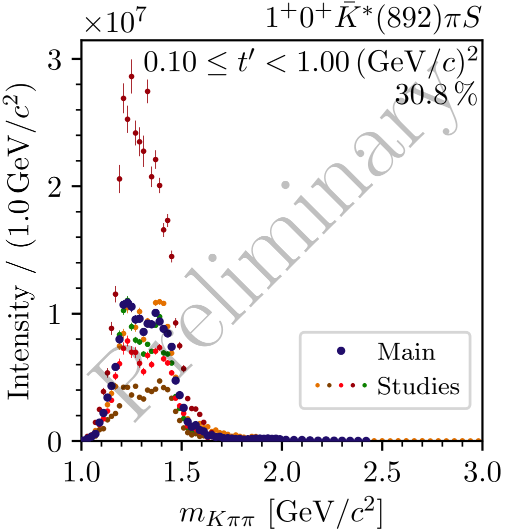

- $K^-\pi^-\pi^+$ and $\pi^-\pi^-\pi^+$ similar experimental footprint
- Distinguishable only by
  - Beam particle identification
  - Final-state particle identification
- Excellent beam PID:
  - Expect small contamination from beam π^-
- Final-state PID does not suppress $\pi^-\pi^-\pi^+$ background
  - ➥ Non-negligible $\pi^-\pi^-\pi^+$ background in $K^-\pi^-\pi^+$ sample of about 7 %
  - ➥ Dominant background in $K^-\pi^-\pi^+$ sample

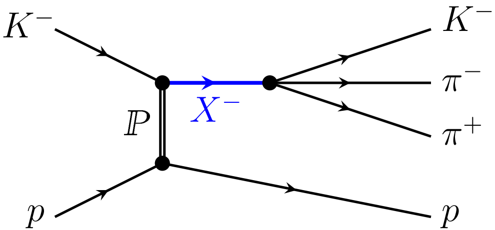

- $K^-\pi^-\pi^+$ and $\pi^-\pi^-\pi^+$ similar experimental footprint
- Distinguishable only by
  - Beam particle identification
  - Final-state particle identification
- Excellent beam PID:
  - Expect small contamination from beam π^-
- Final-state PID does not suppress $\pi^-\pi^-\pi^+$ background
  - ➥ Non-negligible $\pi^-\pi^-\pi^+$ background in $K^-\pi^-\pi^+$ sample of about 7 %
  - ➥ Dominant background in $K^-\pi^-\pi^+$ sample

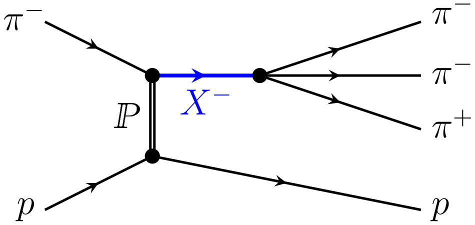

- $K^-\pi^-\pi^+$ and $\pi^-\pi^-\pi^+$ similar experimental footprint
- Distinguishable only by
  - Beam particle identification
  - Final-state particle identification
- Excellent beam PID:
  - Expect small contamination from beam π^-
- Final-state PID does not suppress $\pi^-\pi^-\pi^+$ background
  - ➥ Non-negligible $\pi^-\pi^-\pi^+$ background in $K^-\pi^-\pi^+$ sample of about 7 %
  - ➥ Dominant background in $K^-\pi^-\pi^+$ sample

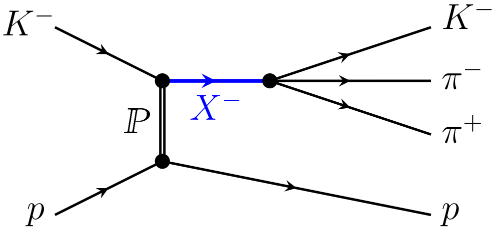

- $K^-\pi^-\pi^+$ and $\pi^-\pi^-\pi^+$ similar experimental footprint
- Distinguishable only by
  - Beam particle identification
  - Final-state particle identification
- Excellent beam PID:
  - Expect small contamination from beam π^-
- Final-state PID does not suppress $\pi^-\pi^-\pi^+$ background
  - ➥ Non-negligible $\pi^-\pi^-\pi^+$ background in $K^-\pi^-\pi^+$ sample of about 7 %
  - ➥ Dominant background in $K^-\pi^-\pi^+$ sample

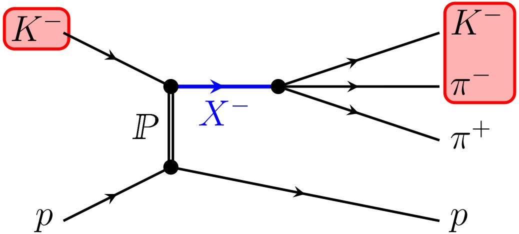

[Phys. Rev. D 95 (2017) 032004]

- Well established model for $\pi^- + p \to \pi^-\pi^-\pi^+ + p$
  - From very same data set
  - Measured with high precision
  - Acceptance corrected
- Generate $\pi^-\pi^-\pi^+$ Monte Carlo sample
- Mis-interpret $\pi^-\pi^-\pi^+$ Monte Carlo events as $K^-\pi^-\pi^+$
  - Apply wrong mass assumption
  - Same event reconstruction and selection as for $K^-\pi^-\pi^+$
- Perform partial-wave decomposition of mis-interpreted $\pi^-\pi^-\pi^+$ Monte Carlo sample
  - Using the same PWA model as for measured $K^-\pi^-\pi^+$ sample

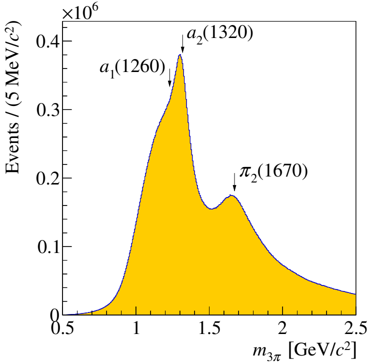

Incoherent Background

[Phys. Rev. D 95 (2017) 032004]

- Well established model for $\pi^- + p \to \pi^-\pi^-\pi^+ + p$
  - From very same data set
  - Measured with high precision
  - Acceptance corrected
- Generate $\pi^-\pi^-\pi^+$ Monte Carlo sample
- Mis-interpret $\pi^-\pi^-\pi^+$ Monte Carlo events as $K^-\pi^-\pi^+$
  - Apply wrong mass assumption
  - Same event reconstruction and selection as for $K^-\pi^-\pi^+$
- Perform partial-wave decomposition of mis-interpreted $\pi^-\pi^-\pi^+$ Monte Carlo sample
  - Using the same PWA model as for measured $K^-\pi^-\pi^+$ sample

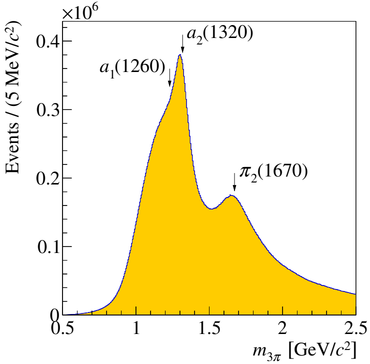

- Well established model for $\pi^- + p \to \pi^-\pi^-\pi^+ + p$
  - From very same data set
  - Measured with high precision
  - Acceptance corrected
- Generate $\pi^-\pi^-\pi^+$ Monte Carlo sample
- Mis-interpret $\pi^-\pi^-\pi^+$ Monte Carlo events as $K^-\pi^-\pi^+$
  - Apply wrong mass assumption
  - Same event reconstruction and selection as for $K^-\pi^-\pi^+$
- Perform partial-wave decomposition of mis-interpreted $\pi^-\pi^-\pi^+$ Monte Carlo sample
  - Using the same PWA model as for measured $K^-\pi^-\pi^+$ sample

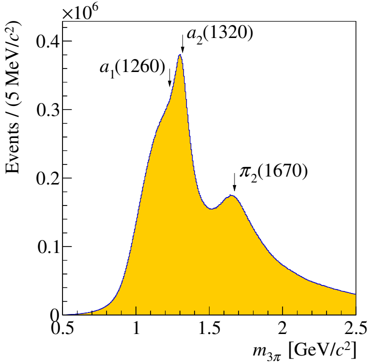

- Well established model for $\pi^- + p \to \pi^-\pi^-\pi^+ + p$
  - From very same data set
  - Measured with high precision
  - Acceptance corrected
- Generate $\pi^-\pi^-\pi^+$ Monte Carlo sample
- Mis-interpret $\pi^-\pi^-\pi^+$ Monte Carlo events as $K^-\pi^-\pi^+$
  - Apply wrong mass assumption
  - Same event reconstruction and selection as for $K^-\pi^-\pi^+$
- Perform partial-wave decomposition of mis-interpreted $\pi^-\pi^-\pi^+$ Monte Carlo sample
  - Using the same PWA model as for measured $K^-\pi^-\pi^+$ sample

➥ Study $\pi^-\pi^-\pi^+$ background in individual $K^-\pi^-\pi^+$ partial waves

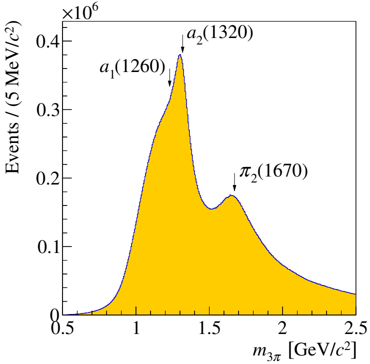

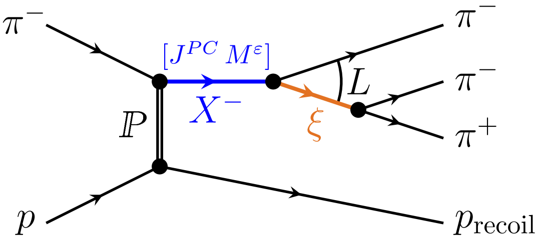

Challenge

Need knowledge of isobar amplitude to calculate decay amplitudes $\Psi_a(\tau)$

- How good are the parameterizations?
  - Single isobar may not be approximated well by a Breit-Wigner amplitude
  - Effects of rescattering may distort the isobar shape

Freed-Isobar Method

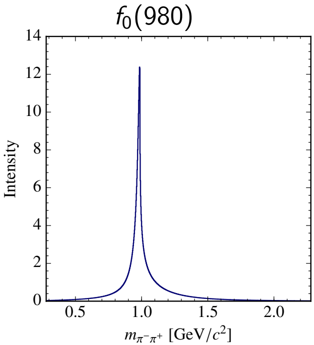

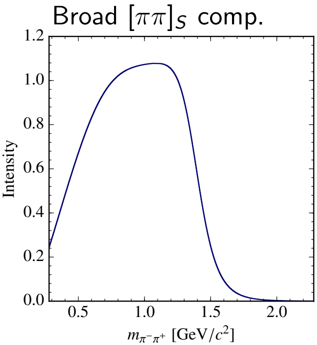

Challenge

Need knowledge of isobar amplitude to calculate decay amplitudes $\Psi_a(\tau)$

- How good are the parameterizations?
  - Single isobar may not be approximated well by a Breit-Wigner amplitude
  - Effects of rescattering may distort the isobar shape

Freed-Isobar Method

$[\pi\pi]_S$ isobar amplitude

Extract isobar amplitudes from data

- Replace model for isobar amplitude with step-like amplitude
- Extract binned shape from data
- Computationally more expensive
  - Up to 100 additional parameters per wave with freed isobar
- Needs large data sets

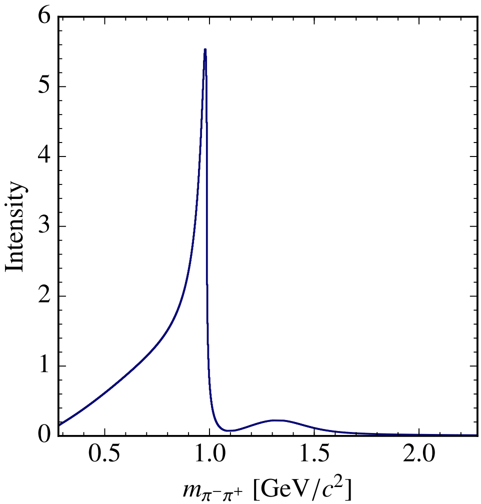

$[\pi\pi]_S$ isobar amplitude

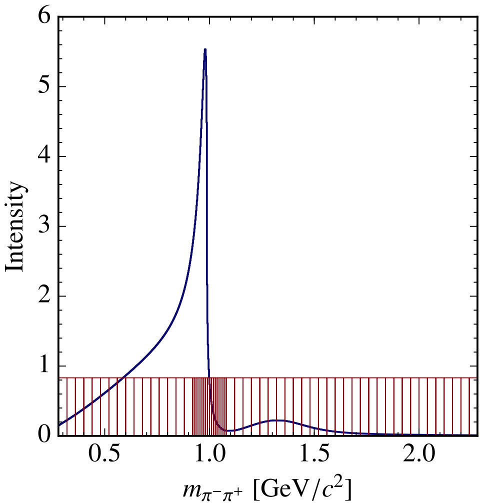

Extract isobar amplitudes from data

- Replace model for isobar amplitude with step-like amplitude
- Extract binned shape from data
- Computationally more expensive
  - Up to 100 additional parameters per wave with freed isobar
- Needs large data sets

Freed-Isobar Method

Extract isobar amplitudes from data

- Replace model for isobar amplitude with step-like amplitude
- Extract binned shape from data
- Computationally more expensive
  - Up to 100 additional parameters per wave with freed isobar
- Needs large data sets

$[\pi\pi]_S$ isobar amplitude

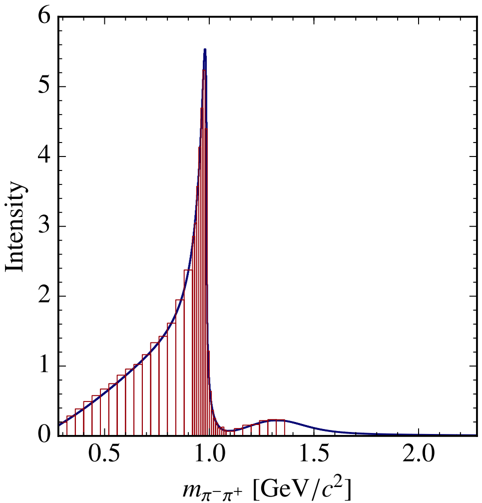

Freed-Isobar Method

Extract isobar amplitudes from data

- Replace model for isobar amplitude with step-like amplitude
- Extract binned shape from data
- Computationally more expensive
  - Up to 100 additional parameters per wave with freed isobar
- Needs large data sets

$[\pi\pi]_S$ isobar amplitude

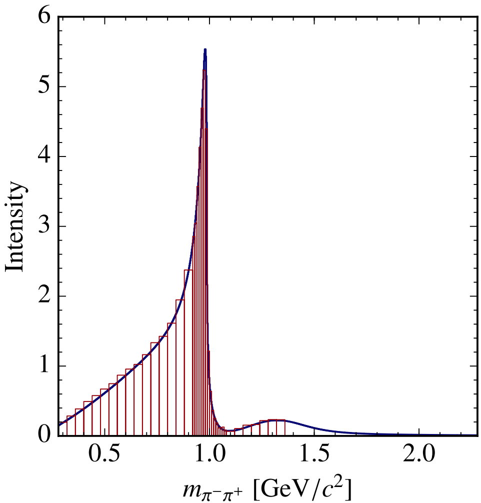

Freed-Isobar Method

$[\pi\pi]_S$ isobar amplitude

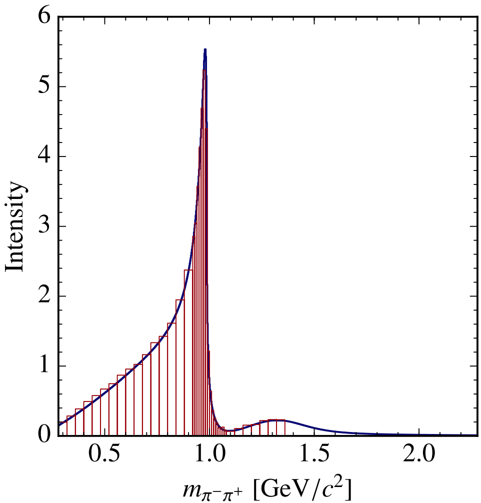

Extract isobar amplitudes from data

- Replace model for isobar amplitude with step-like amplitude
- Extract binned shape from data
- Computationally more expensive
  - Up to 100 additional parameters per wave with freed isobar
- Needs large data sets

Freed-Isobar Method

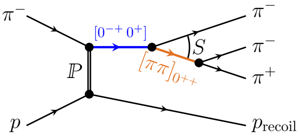

Example: $0^{-+}\,0^+\,[\pi\pi\ S\text{-wave}]\,\pi\,S$ wave

- Comparison of $0^{-+}\,0^+\,[\pi\pi\ S\text{-wave}]\,\pi\,S$ wave intensity between
  - sum of all conventional isobar waves
  - freed-isobar method
- Compatible shapes
- $\pi(1800)$ peak prominent

Freed-Isobar Method

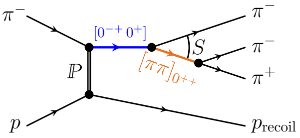

Example: $0^{-+}\,0^+\,[\pi\pi\ S\text{-wave}]\,\pi\,S$ wave

- Comparison of $0^{-+}\,0^+\,[\pi\pi\ S\text{-wave}]\,\pi\,S$ wave intensity between
  - sum of all conventional isobar waves
  - freed-isobar method
- Compatible shapes
- $\pi(1800)$ peak prominent

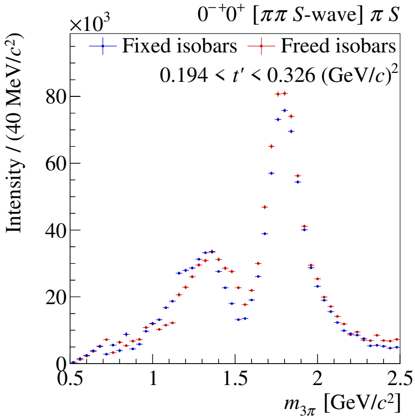

Freed-Isobar Method

[Adolph et al., PRD 95, 032004 (2017)]

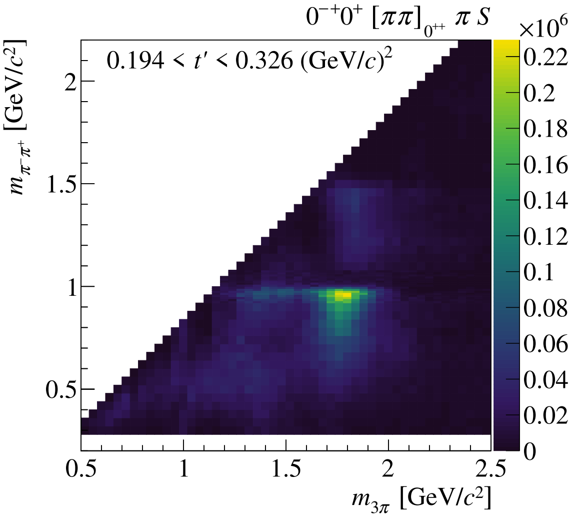

This is not a Dalitz-plot

[Adolph et al., PRD 95, 032004 (2017)]

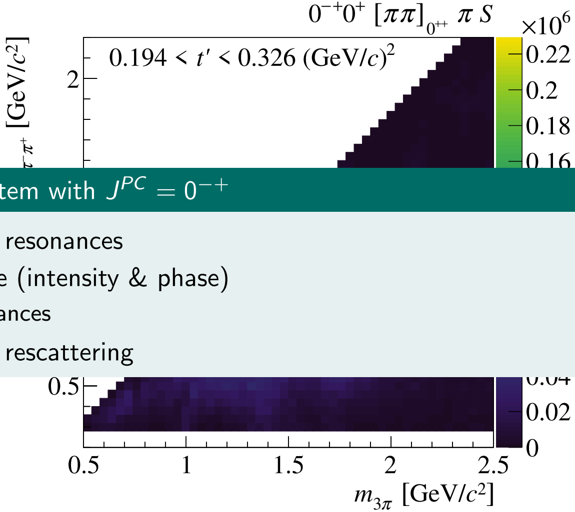

Investigate the $\pi\pi$ subsystem with $J^{PC} = 0^{-+}$

- No constrains on $\pi\pi$ resonances
- Extract $\pi\pi$ amplitude (intensity & phase)
  - Extract $\pi\pi$ resonances
- Investigate effects of rescattering

This is not a Dalitz-plot

Freed-Isobar Method: $0^{-+}\,0^{+}\,[\pi\pi]_{0^{++}}\,\pi\,S$

[Adolph et al., PRD 95, 032004 (2017)]

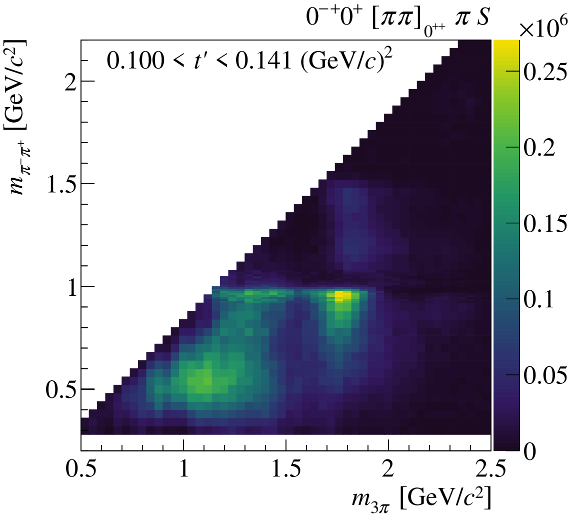

This is not a Dalitz-plot

Freed-Isobar Method: $0^{-+}\,0^{+}\,[\pi\pi]_{0^{++}}\,\pi\,S$

[Adolph et al., PRD 95, 032004 (2017)]

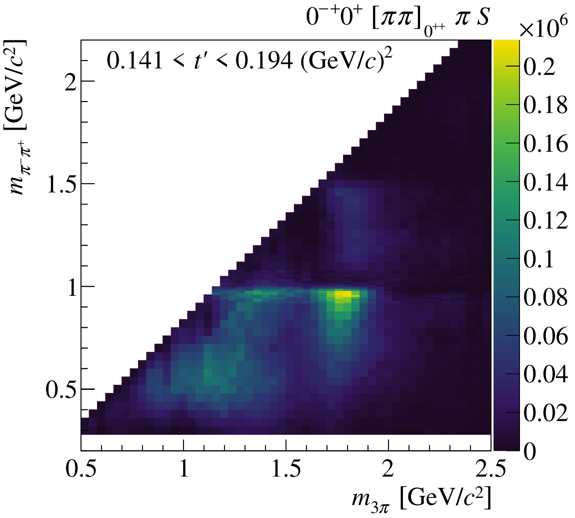

This is not a Dalitz-plot

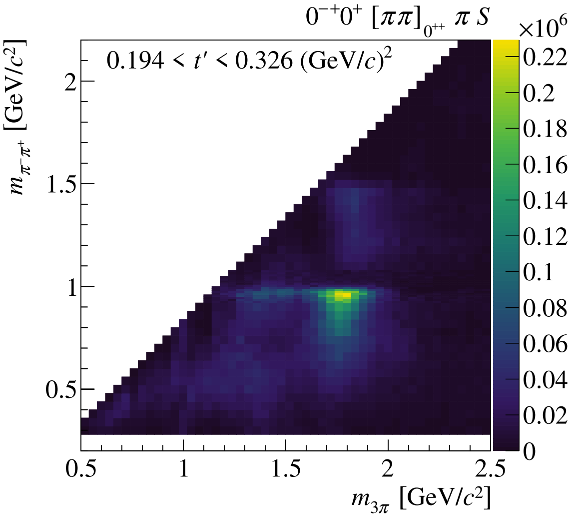

This is not a Dalitz-plot

Freed-Isobar Method: $0^{-+}\,0^{+}\,[\pi\pi]_{0^{++}}\,\pi\,S$

[Adolph et al., PRD 95, 032004 (2017)]

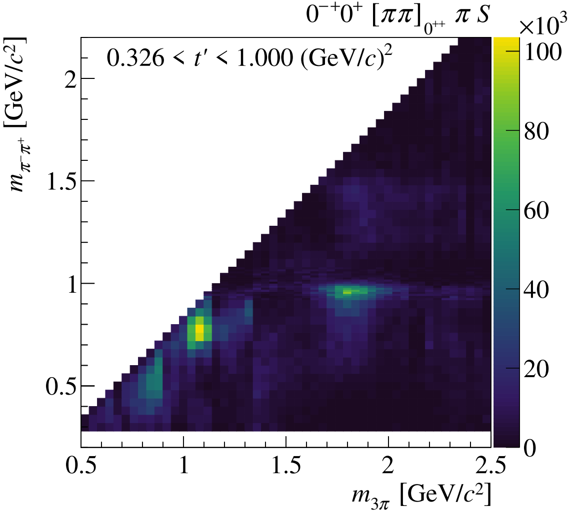

This is not a Dalitz-plot

Freed-Isobar Method: $0^{-+}\,0^{+}\,[\pi\pi]_{0^{++}}\,\pi\,S$

[Adolph et al., PRD 95, 032004 (2017)]

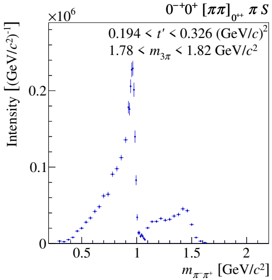

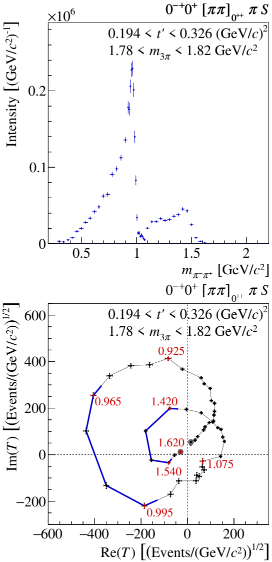

0⁻⁺0⁺ [ππ]0⁺⁺ π S
×10⁶
0.194 < t′ < 0.326 (GeV/c)²
1.78 < m3π < 1.82 GeV/c²
Intensity [(GeV/c²)⁻¹]
0.2
0.1
0
0.5
1
1.5
2
mπ⁻π⁺ [GeV/c²]
0⁻⁺0⁺ [ππ]0⁺⁺ π S
0.194 < t′ < 0.326 (GeV/c)²
1.78 < m3π < 1.82 GeV/c²
0.925
0.965
1.420
1.620
1.075
1.540
0.995
Im(T) [(Events/(GeV/c²))^1/2]
600
400
200
0
−200
−600
−400
−200
0
200
Re(T) [(Events/(GeV/c²))^1/2]

Freed-Isobar Method

Freed-Isobar Method: $0^{-+}\,0^{+}\,[\pi\pi]_{0^{++}}\,\pi\,S$

[Adolph et al., PRD 95, 032004 (2017)]

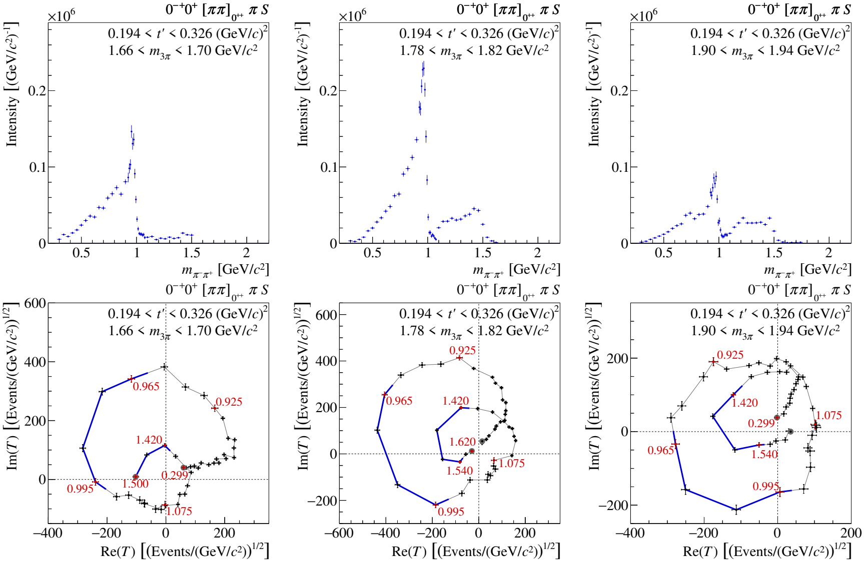

- Total intensity in one $(m_{3\pi}, t')$-bin as function of phase-space variables $\vec{\tau}$:

$$\mathcal{I}(\vec{\tau}) = \left| \sum_{i}^{\text{waves}} \mathcal{T}_i \left[\psi_i(\vec{\tau})\, \Delta_i(m_{\pi^-\pi^+}) + \text{Bose Symm.} \right] \right|^2$$

Fit parameters: Production amplitudes $\mathcal{T}_i$

Fixed: Angular distributions $\psi_i(\vec{\tau})$, dynamic isobar amplitudes $\Delta_i(m_{\pi^-\pi^+})$

- Replace fixed isobar amplitudes by piece-wise constant function:

$$\Delta_i(m_{\pi^-\pi^+}) \to \sum_{\text{bins}} \mathscr{T}_i^{\text{bin}} \Delta_i^{\text{bin}}(m_{\pi^-\pi^+}) \equiv [\pi\pi]_{J^{PC}}$$

$$\Delta_i^{\text{bin}}(m_{\pi^-\pi^+}) = \begin{cases} 1, & \text{if } m_{\pi^-\pi^+} \text{ in the bin.} \\ 0, & \text{otherwise.} \end{cases}$$

- Each $m_{\pi^-\pi^+}$ bin behaves like an independent partial wave $\mathcal{T}_i^{\text{bin}} = \mathcal{T}_i \mathscr{T}_i^{\text{bin}}$:

$$\mathcal{I}(\vec{\tau}) = \left| \sum_{i}^{\text{waves}} \sum_{\text{bin}}^{\text{bins}} \mathcal{T}_i^{\text{bin}} \left[\psi_i(\vec{\tau})\, \Delta_i^{\text{bin}}(m_{\pi^-\pi^+}) + \text{Bose Symm.} \right] \right|^2$$

- Approach similar to binning in $m_{3\pi}$

- Extend freed-isobar wave set
- Free isobar dynamic amplitudes of 11 biggest waves:
  - Minimize potential leakage

Freed-isobar wave set

$0^{-+}0^{+}[\pi\pi]_{0^{++}}\pi S$	$1^{++}1^{+}[\pi\pi]_{1^{--}}\pi S$	$2^{-+}0^{+}[\pi\pi]_{2^{++}}\pi S$
$0^{-+}0^{+}[\pi\pi]_{1^{--}}\pi P$	$2^{-+}0^{+}[\pi\pi]_{0^{++}}\pi D$	$2^{-+}1^{+}[\pi\pi]_{1^{--}}\pi P$
$1^{++}0^{+}[\pi\pi]_{0^{++}}\pi P$	$2^{-+}0^{+}[\pi\pi]_{1^{--}}\pi P$	$2^{++}1^{+}[\pi\pi]_{1^{--}}\pi D$
$1^{++}0^{+}[\pi\pi]_{1^{--}}\pi S$	$2^{-+}0^{+}[\pi\pi]_{1^{--}}\pi F$	

- Extend freed-isobar wave set
- Free isobar dynamic amplitudes of 11 biggest waves:
  - Minimize potential leakage
- Add spin exotic $1^{-+}1^{+}[\pi\pi]_{1^{--}}\pi P$ wave
  - Wave of major interest
- 12 freed-isobar waves replace 16 fixed-isobar waves
- In addition 72 fixed-isobar waves in the model
- 40 MeV wide $m_{3\pi}$ bins from 0.5 to 2.5 GeV
- 4 non-equidistant bins in t'
- 50 bins in $m_{3\pi}$, 4 bins in t': $4 \times 50 = 200$ independent bins

- Freed-isobar analysis: much more freedom than fixed-isobar analysis
  - Causes continuous mathematical ambiguities in the model
- "Zero mode" = dynamic isobar amplitude $\Omega\left(m_{\pi^-\pi^+}\right)$, that does not contribute to the **total** amplitude
- Spin-exotic wave:

$$\psi\left(\vec{\tau}\right)\Omega\left(m_{\pi^-\pi^+}\right) + \text{Bose Symm.} = 0$$

at **every point** $\vec{\tau}$ in phase space

- Process: $X^- \to \xi\pi_3^- \to \pi_1^-\pi_2^+\pi_3^-$.
- Condition for zero mode at all points $\vec{\tau}$ in phase-space:

$$\psi\left(\vec{\tau}_{123}\right)\,\Omega\left(m_{12}\right) + \text{Bose Symm.} = 0 \qquad (1)$$

- Tensor formalism with pion momenta defined in the X^- rest frame:

$$\psi\left(\vec{\tau}_{123}\right) \propto \vec{p}_1 \times \vec{p}_3$$

- Bose symmetrization ($\pi_1^- \leftrightarrow \pi_3^-$):

$$\vec{p}_1 \times \vec{p}_3\,\Omega\left(m_{12}\right) + \vec{p}_3 \times \vec{p}_1\,\Omega\left(m_{23}\right) = \vec{p}_1 \times \vec{p}_3\left[\Omega\left(m_{12}\right) - \Omega\left(m_{23}\right)\right]$$

  - Fulfill eq. (1) at every point in phase space $\Rightarrow \Omega\left(m_\xi\right) = \text{const.}$

- If $\Omega\left(m_\xi\right)$ is added to the physical dynamic isobar amplitude $\Delta^{\text{phys}}\left(m_\xi\right)$, the total amplitude, and thus the intensity, is not altered:

$$\left|\psi\left(\vec{\tau}\right)\Delta^{\text{phys}}\left(m_\xi\right) + \text{B. S.}\right|^2 = \left|\psi\left(\vec{\tau}\right)\left[\Delta^{\text{phys}}\left(m_\xi\right) + \mathcal{C}\Omega\left(m_\xi\right)\right] + \text{B. S.}\right|^2$$

  for any complex-valued zero-mode coefficient $\mathcal{C}$
- $\mathcal{C}$: complex-valued ambiguity in the model

$$\Delta_{\mathrm{BW}}\left(m_{\pi^-\pi^+}\right) + \mathcal{C}\Omega\left(m_{\pi^-\pi^+}\right) \quad (2)$$

$\mathcal{C} = 0.00 + 0.00i$

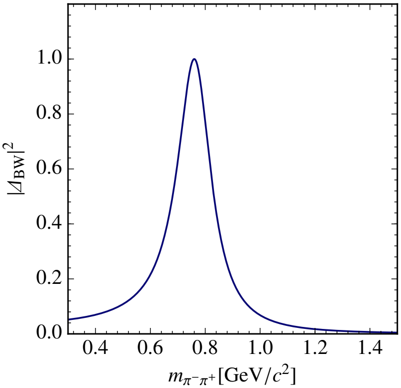

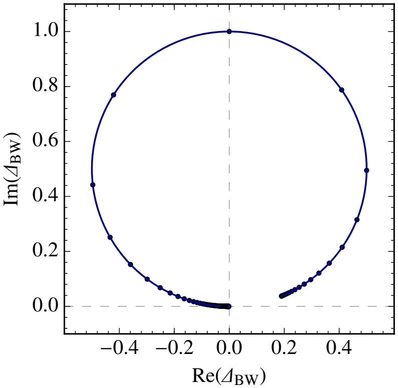

All amplitudes describe the same intensity

$$\Delta_{\mathrm{BW}}\left(m_{\pi^-\pi^+}\right) + \mathcal{C}\Omega\left(m_{\pi^-\pi^+}\right) \tag{2}$$

$$\mathcal{C} = -0.01 + 0.08i$$

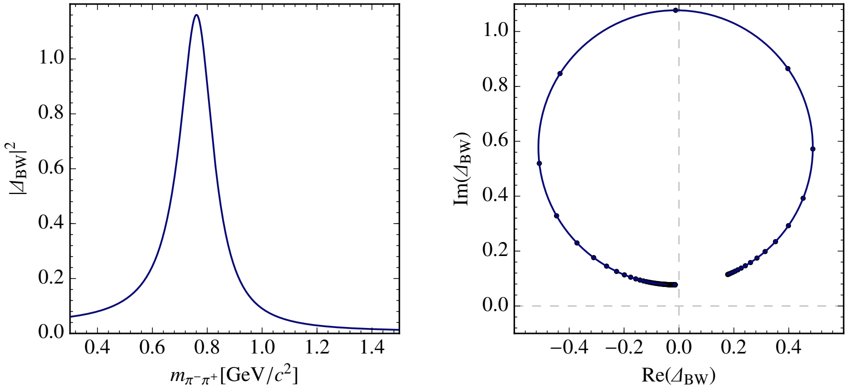

All amplitudes describe the same intensity

$$\Delta_{\text{BW}}\left(m_{\pi^-\pi^+}\right) + \mathcal{C}\Omega\left(m_{\pi^-\pi^+}\right) \tag{2}$$

$\mathcal{C} = -0.05 + 0.15i$

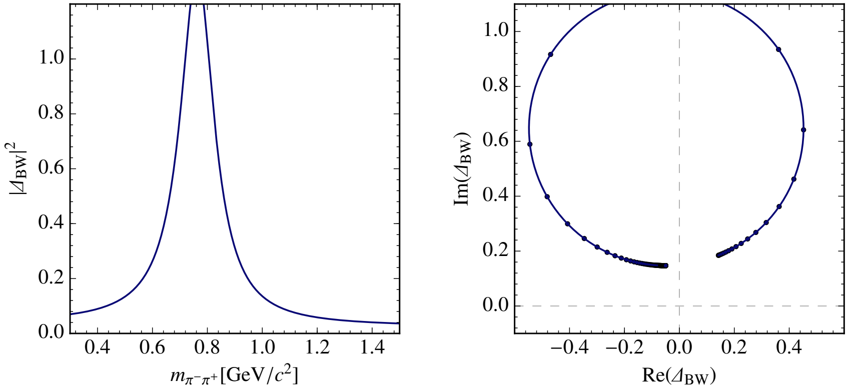

All amplitudes describe the same intensity

$$\Delta_{\mathrm{BW}}\left(m_{\pi^-\pi^+}\right) + \mathcal{C}\Omega\left(m_{\pi^-\pi^+}\right) \quad (2)$$

$$\mathcal{C} = -0.10 + 0.20i$$

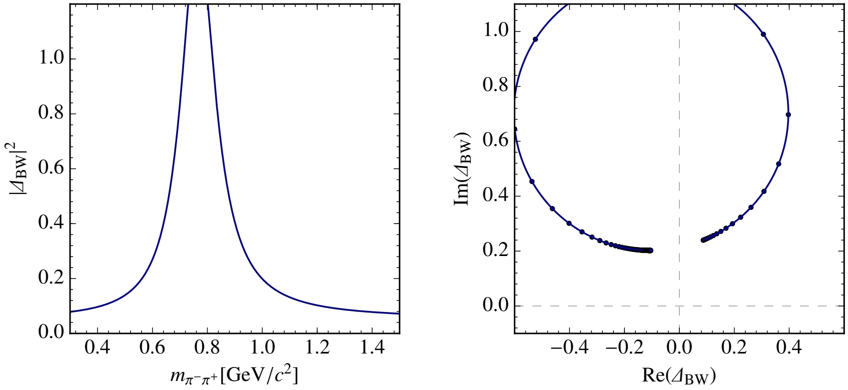

All amplitudes describe the same intensity

$$\Delta_{\mathrm{BW}}\left(m_{\pi^-\pi^+}\right) + \mathcal{C}\Omega\left(m_{\pi^-\pi^+}\right) \tag{2}$$

$$\mathcal{C} = -0.17 + 0.24i$$

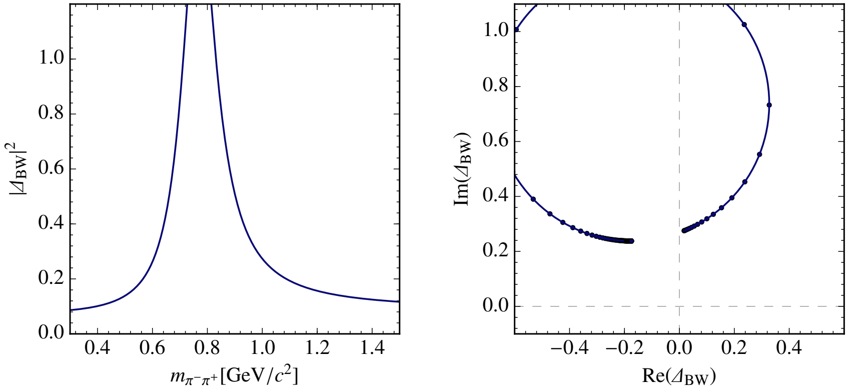

All amplitudes describe the same intensity

$$\Delta_{\mathrm{BW}}\left(m_{\pi^-\pi^+}\right) + \mathcal{C}\Omega\left(m_{\pi^-\pi^+}\right) \tag{2}$$

$$\mathcal{C} = -0.25 + 0.25i$$

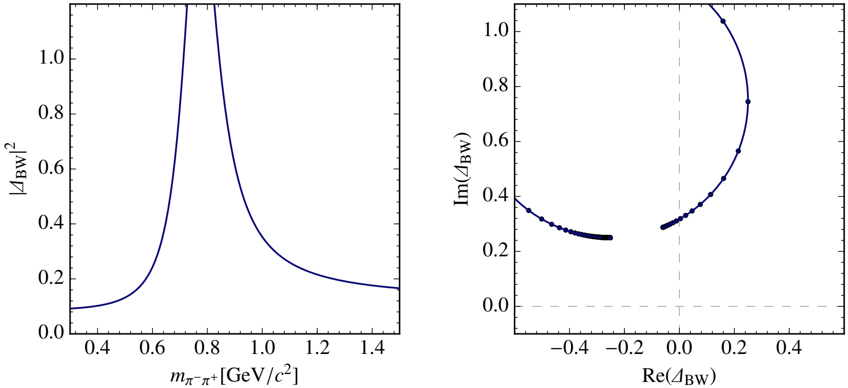

All amplitudes describe the same intensity

$$\Delta_{\text{BW}}\left(m_{\pi^-\pi^+}\right) + \mathcal{C}\Omega\left(m_{\pi^-\pi^+}\right) \quad (2)$$

$$\mathcal{C} = -0.33 + 0.24i$$

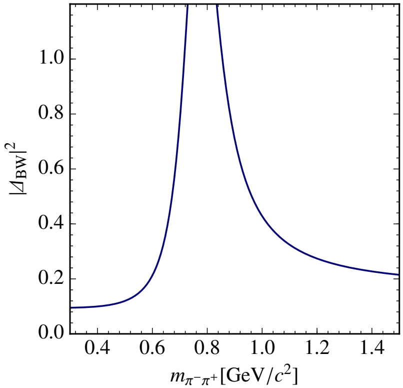

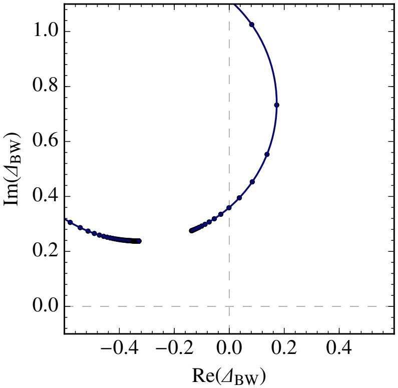

All amplitudes describe the same intensity

$$\Delta_{\text{BW}}\left(m_{\pi^-\pi^+}\right) + \mathcal{C}\Omega\left(m_{\pi^-\pi^+}\right) \quad (2)$$

$\mathcal{C} = -0.40 + 0.20i$

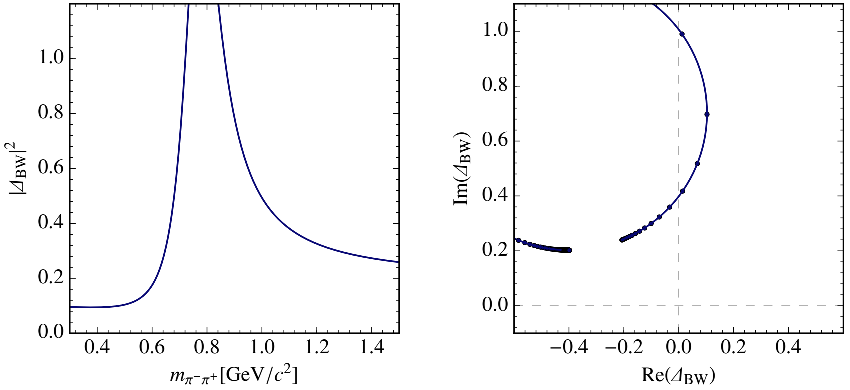

All amplitudes describe the same intensity

$$\Delta_{\mathrm{BW}}\left(m_{\pi^-\pi^+}\right) + \mathcal{C}\Omega\left(m_{\pi^-\pi^+}\right) \tag{2}$$

$\mathcal{C} = -0.45 + 0.15i$

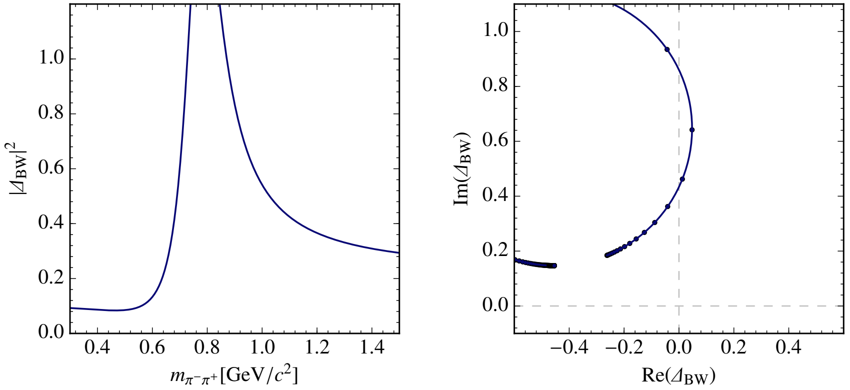

All amplitudes describe the same intensity

$$\Delta_{\mathrm{BW}}\left(m_{\pi^-\pi^+}\right) + \mathcal{C}\Omega\left(m_{\pi^-\pi^+}\right) \tag{2}$$

$\mathcal{C} = -0.49 + 0.08i$

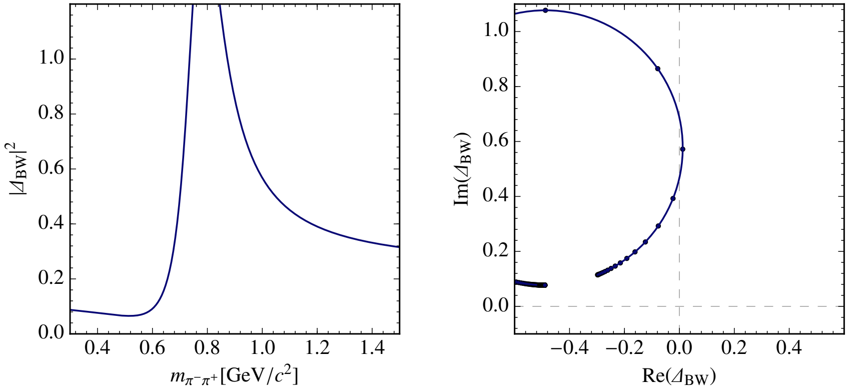

All amplitudes describe the same intensity

$$\Delta_{\mathrm{BW}}\left(m_{\pi^-\pi^+}\right) + \mathcal{C}\Omega\left(m_{\pi^-\pi^+}\right) \tag{2}$$

$\mathcal{C} = -0.50 + 0.00i$

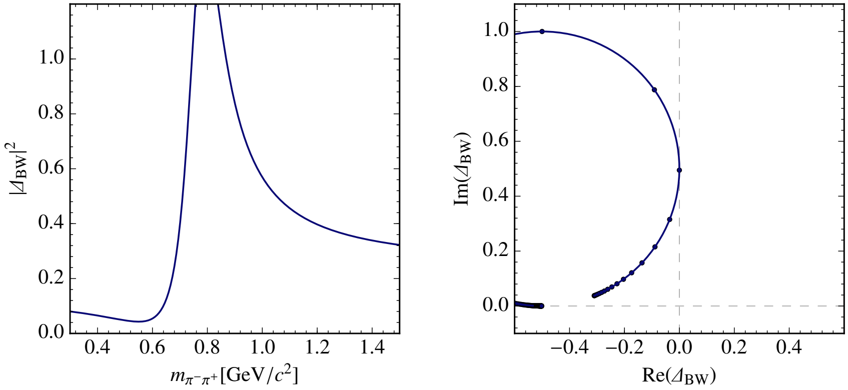

All amplitudes describe the same intensity

$$\Delta_{\mathrm{BW}}\left(m_{\pi^-\pi^+}\right) + \mathcal{C}\Omega\left(m_{\pi^-\pi^+}\right) \tag{2}$$

$\mathcal{C} = -0.49 - 0.08i$

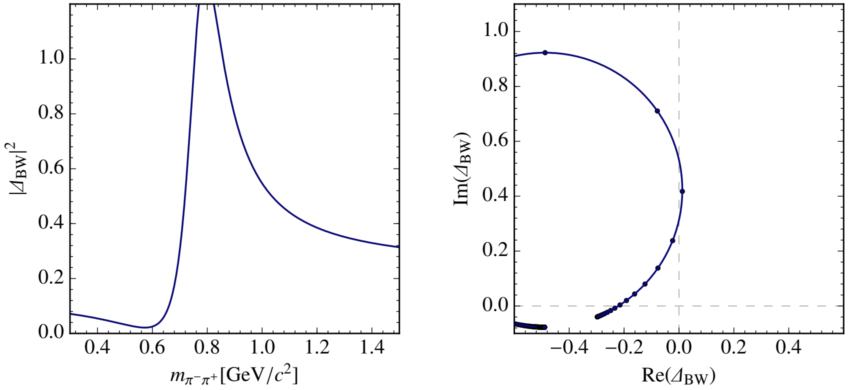

All amplitudes describe the same intensity

$$\Delta_{\mathrm{BW}}\left(m_{\pi^-\pi^+}\right) + \mathcal{C}\Omega\left(m_{\pi^-\pi^+}\right) \quad (2)$$

$$\mathcal{C} = -0.45 - 0.15i$$

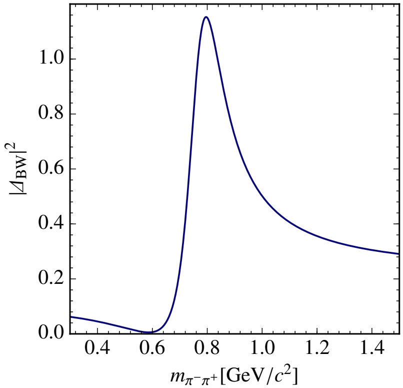

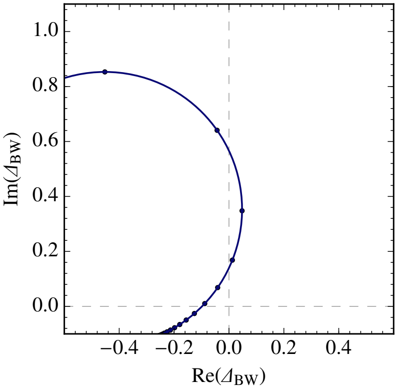

All amplitudes describe the same intensity

$$\Delta_{\mathrm{BW}}\left(m_{\pi^-\pi^+}\right) + \mathcal{C}\Omega\left(m_{\pi^-\pi^+}\right) \quad (2)$$

$\mathcal{C} = -0.40 - 0.20i$

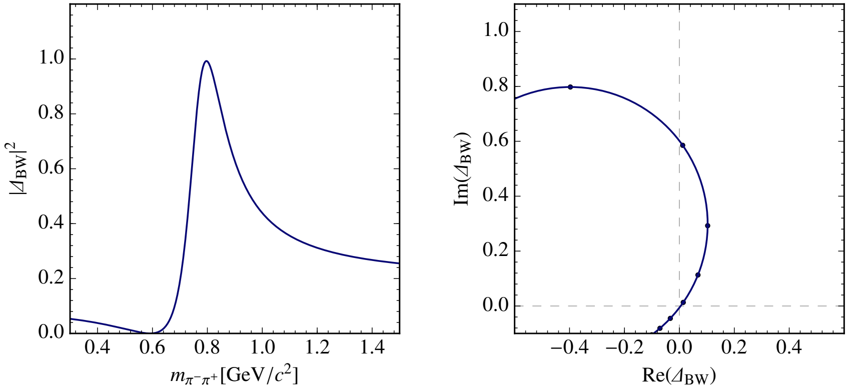

All amplitudes describe the same intensity

$$\Delta_{\mathrm{BW}}\left(m_{\pi^-\pi^+}\right) + \mathcal{C}\Omega\left(m_{\pi^-\pi^+}\right) \quad (2)$$

$\mathcal{C} = -0.33 - 0.24i$

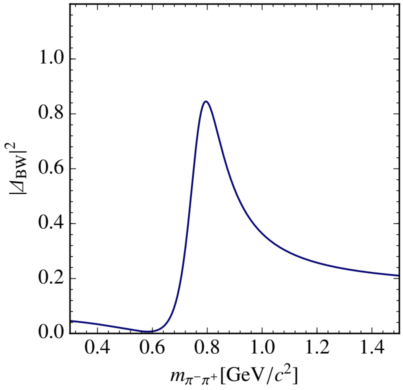

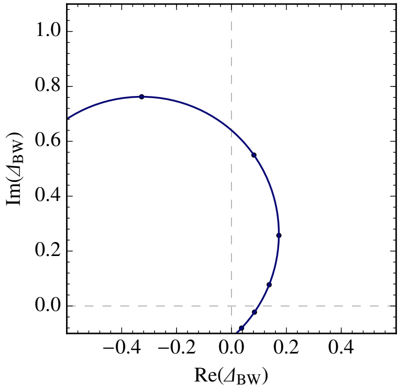

All amplitudes describe the same intensity

$$\Delta_{\mathrm{BW}}\left(m_{\pi^-\pi^+}\right) + \mathcal{C}\Omega\left(m_{\pi^-\pi^+}\right) \quad (2)$$

$\mathcal{C} = -0.25 - 0.25i$

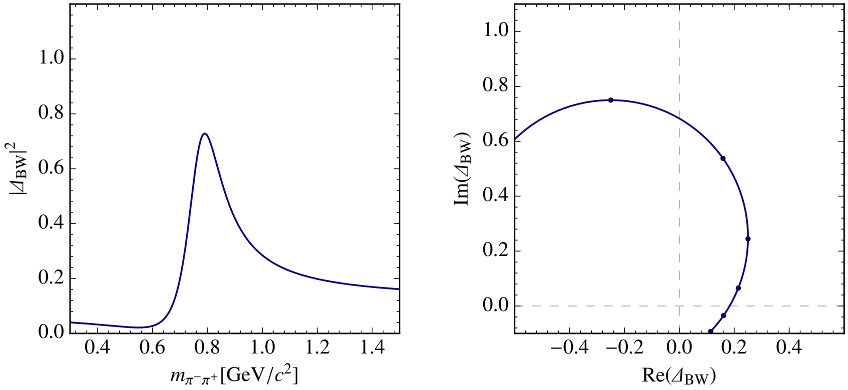

All amplitudes describe the same intensity

$$\Delta_{\mathrm{BW}}\left(m_{\pi^-\pi^+}\right) + \mathcal{C}\Omega\left(m_{\pi^-\pi^+}\right) \tag{2}$$

$\mathcal{C} = -0.17 - 0.24i$

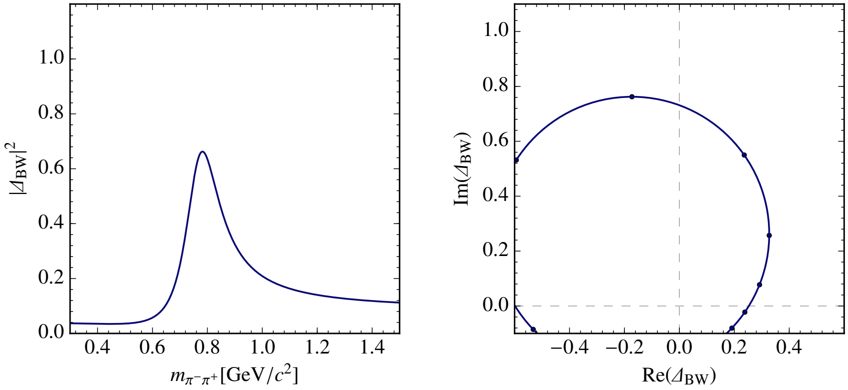

All amplitudes describe the same intensity

$$\Delta_{\text{BW}}\left(m_{\pi^-\pi^+}\right) + \mathcal{C}\Omega\left(m_{\pi^-\pi^+}\right) \tag{2}$$

$$\mathcal{C} = -0.10 - 0.20i$$

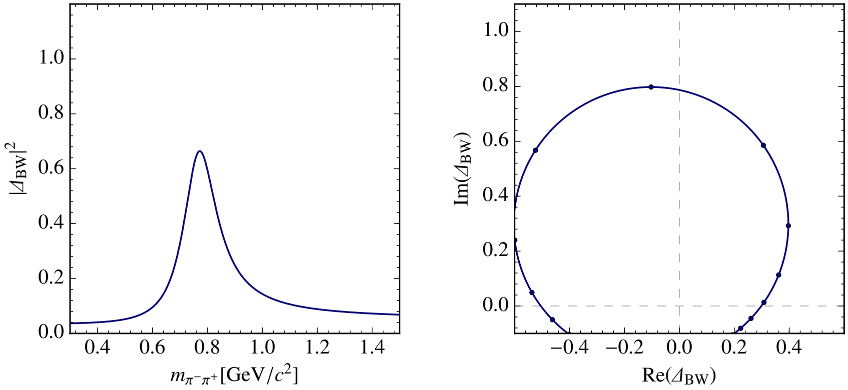

All amplitudes describe the same intensity

$$\Delta_{\mathrm{BW}}\left(m_{\pi^-\pi^+}\right) + \mathcal{C}\Omega\left(m_{\pi^-\pi^+}\right) \qquad (2)$$

$\mathcal{C} = -0.05 - 0.15i$

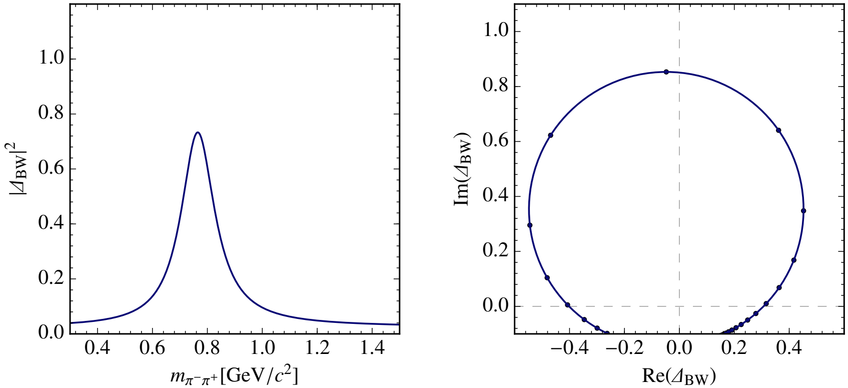

All amplitudes describe the same intensity

$$\Delta_{\mathrm{BW}}\left(m_{\pi^-\pi^+}\right) + \mathcal{C}\Omega\left(m_{\pi^-\pi^+}\right) \tag{2}$$

$\mathcal{C} = -0.01 - 0.08i$

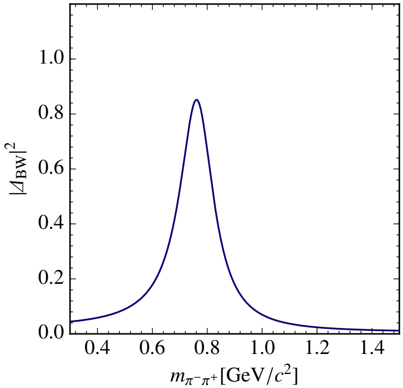

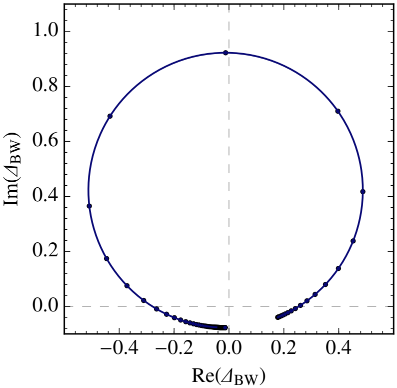

All amplitudes describe the same intensity

$$\Delta_{\text{BW}}\left(m_{\pi^-\pi^+}\right) + \mathcal{C}\Omega\left(m_{\pi^-\pi^+}\right) \tag{2}$$

$\mathcal{C} = 0.00 + 0.00i$

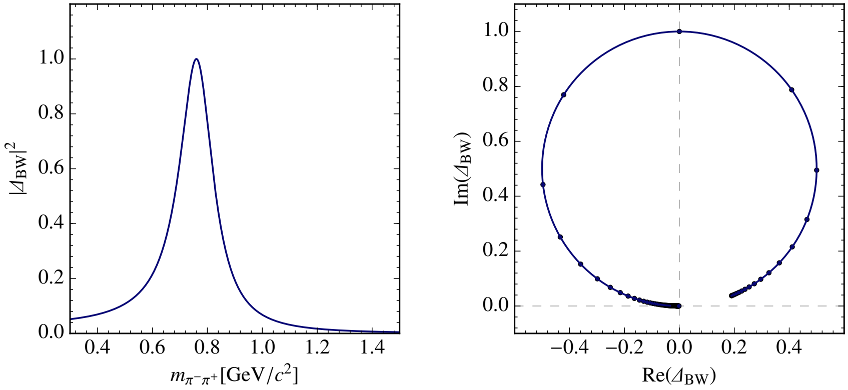

All amplitudes describe the same intensity

- Now for $m_{\pi^-\pi^+}$ bins: $\vec{\mathcal{T}}^0 = \{\Omega(m_{\text{bin}})\}$ for all $m_{\pi^-\pi^+}$bins
- The fitting algorithm might find a solution, shifted away from the physical solution $\vec{\mathcal{T}}^{\text{phys}}$:

$$\vec{\mathcal{T}}^{\text{phys}} = \vec{\mathcal{T}}^{\text{fit}} + \mathcal{C}\vec{\mathcal{T}}^0$$

- Obtain physical solution: constrain $\mathcal{C}$ by conditions on the resulting dynamic amplitudes $\vec{\mathcal{T}}^{\text{fit}}$
- In the case of the $1^{-+}1^+[\pi\pi]_{1^{--}}\pi P$ wave:
  - use the Breit-Wigner for the $\rho(770)$ resonance with fixed resonance parameters as in the fixed-isobar analysis
  - use a Breit-Wigner for the $\rho(770)$ resonance with floating resonance parameters
- Final results: weighted average of these two methods
- **Note:** Resolving the ambiguity fixes only a single complex-valued degree of freedom. $n_{\text{bins}} - 1$ complex-valued degrees of freedom remain free.

The spin-exotic wave

- Example: Single $(m_{3\pi}, t')$ bin
  - $1.58 < m_{3\pi} < 1.62\,\mathrm{GeV}/c^2$
  - $0.326 < t' < 1.000\ (\mathrm{GeV}/c)^2$
- Zero-mode ambiguity resolved with $\rho(770)$ used as constraint

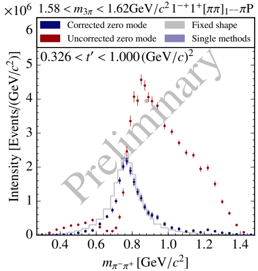

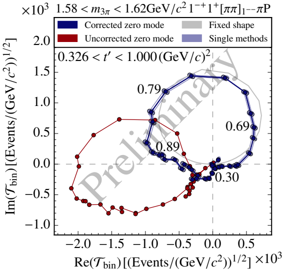

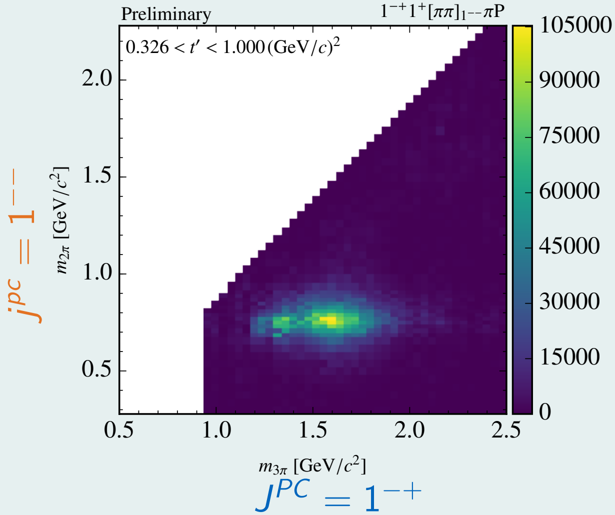
Preliminary
$1^{-+}1^{+}[\pi\pi]_{1^{--}}\pi P$
$0.326 < t' < 1.000\,(\mathrm{GeV}/c)^2$
$m_{2\pi}$ [GeV/c^2]
$m_{3\pi}$ [GeV/c^2]
$j^{pc} = 1^{--}$
$J^{PC} = 1^{-+}$
0.5
1.0
1.5
2.0
2.5
105000
90000
75000
60000
45000
30000
15000
0

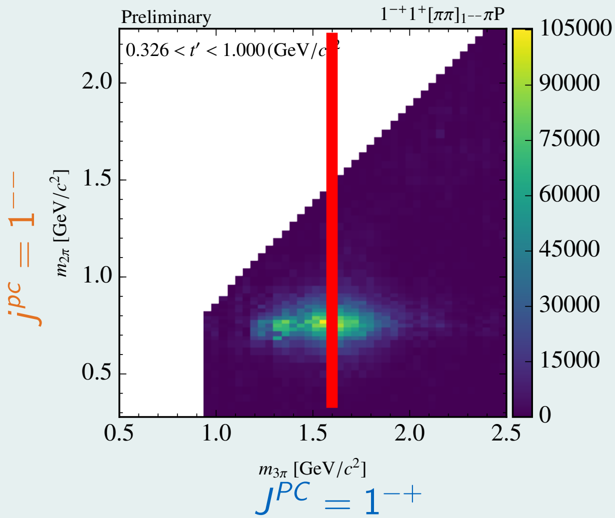

Preliminary
$1^{-+}1^{+}[\pi\pi]_{1^{--}}\pi P$
$0.326 < t' < 1.000\,(\mathrm{GeV}/c^2)$
2.0
1.5
1.0
0.5
$m_{2\pi}$ [GeV/c^2]
0.5
1.0
1.5
2.0
2.5
$m_{3\pi}$ [GeV/c^2]
105000
90000
75000
60000
45000
30000
15000
0
$j^{pc} = 1^{--}$
$J^{PC} = 1^{-+}$

Freed-Isobar Analysis

$J^{PC} = 1^{-+}$ Wave with freed $j^{pc} = 1^{--}$ Isobar Amplitude

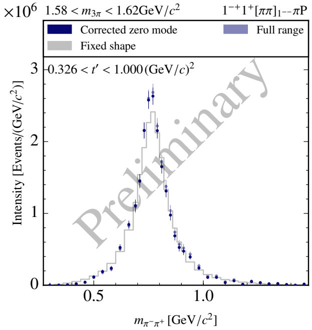

- Study $\pi^-\pi^+$ amplitude as a function of $m_{3\pi}$
- $m_{\pi^-\pi^+}$ spectrum shows good agreement with $\rho(770)$ Breit-Wigner
- Extract $m_{\pi^-\pi^+}$ dependence of complex-valued amplitude
- Shape of $m_{3\pi}$ spectrum is in fair agreement with fixed-isobar analysis
  - ➥ $\pi_1(1600)$ signal at about 1.6 GeV/c^2 robust

Freed-Isobar Analysis

$J^{PC} = 1^{-+}$ Wave with freed $j^{pc} = 1^{--}$ Isobar Amplitude

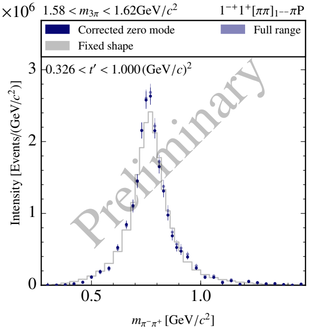

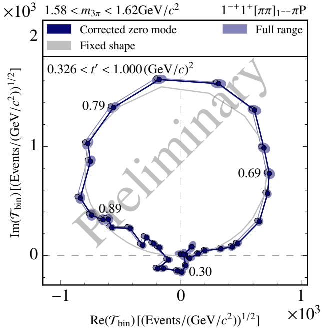

- Study $\pi^-\pi^+$ amplitude as a function of $m_{3\pi}$
- $m_{\pi^-\pi^+}$ spectrum shows good agreement with $\rho(770)$ Breit-Wigner
- Extract $m_{\pi^-\pi^+}$ dependence of complex-valued amplitude
- Shape of $m_{3\pi}$ spectrum is in fair agreement with fixed-isobar analysis
  - ➥ $\pi_1(1600)$ signal at about $1.6 \, \text{GeV}/c^2$ robust

Freed-Isobar Analysis

$J^{PC} = 1^{-+}$ Wave with freed $j^{pc} = 1^{--}$ Isobar Amplitude

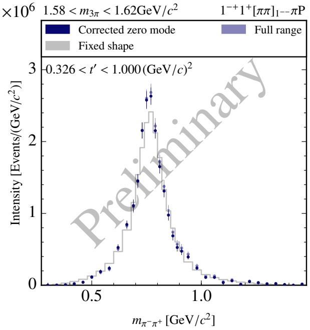

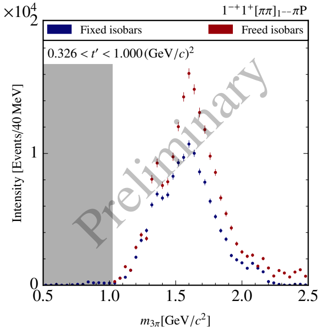

- Study $\pi^-\pi^+$ amplitude as a function of $m_{3\pi}$
- $m_{\pi^-\pi^+}$ spectrum shows good agreement with $\rho(770)$ Breit-Wigner
- Extract $m_{\pi^-\pi^+}$ dependence of complex-valued amplitude
- Shape of $m_{3\pi}$ spectrum is in fair agreement with fixed-isobar analysis
  - ➥ $\pi_1(1600)$ signal at about $1.6\,\text{GeV}/c^2$ robust